



3 4456 0377083 6

oml

ORNL/TM-12437/V1

**OAK RIDGE
NATIONAL
LABORATORY**

MARTIN MARIETTA

**Development of Grout
Formulations for 106-AN Waste:
Mixture-Experiment Results
and Analysis**

**Vol. 1. Narrative and
Recommendations**

R. D. Spence
E. W. McDaniel
Oak Ridge National Laboratory

C. M. Anderson
R. O. Lokken
G. F. Piepel
Pacific Northwest Laboratory

MANAGED BY
MARTIN MARIETTA ENERGY SYSTEMS, INC.
FOR THE UNITED STATES
DEPARTMENT OF ENERGY

OAK RIDGE NATIONAL LABORATORY

CENTRAL RESEARCH LIBRARY

CIRCULATION SECTION

40081 ROOM 173

LIBRARY LOAN COPY

DO NOT TRANSFER TO ANOTHER PERSON

If you wish someone else to see this report, send in request with report and the library will arrange a loan.

This report has been reproduced directly from the best available copy.

Available to DOE and DOE contractors from the Office of Scientific and Technical Information, P.O. Box 62, Oak Ridge, TN 37831; prices available from (615) 576-8401, FTS 626-8401.

Available to the public from the National Technical Information Service, U.S. Department of Commerce, 5285 Port Royal Rd., Springfield, VA 22161.

This report was prepared as an account of work sponsored by an agency of the United States Government. Neither the United States Government nor any agency thereof, nor any of their employees, makes any warranty, express or implied, or assumes any legal liability or responsibility for the accuracy, completeness, or usefulness of any information, apparatus, product, or process disclosed, or represents that its use would not infringe privately owned rights. Reference herein to any specific commercial product, process, or service by trade name, trademark, manufacturer, or otherwise, does not necessarily constitute or imply its endorsement, recommendation, or favoring by the United States Government or any agency thereof. The views and opinions of authors expressed herein do not necessarily state or reflect those of the United States Government or any agency thereof.

**DEVELOPMENT OF GROUT FORMULATIONS FOR 106-AN WASTE:
MIXTURE-EXPERIMENT RESULTS AND ANALYSIS**

VOL. 1. NARRATIVE AND RECOMMENDATIONS

R. D. Spence
E. W. McDaniel
Chemical Technology Division

C. M. Anderson
R. O. Lokken
G. F. Piepel
Pacific Northwest Laboratory^a

Date Published—September 1993

Prepared for
Westinghouse Hanford Company
(Activity No. EW 1010 03 0)

Prepared by
OAK RIDGE NATIONAL LABORATORY
Oak Ridge, Tennessee 37831
managed by
MARTIN MARIETTA ENERGY SYSTEMS, INC.
for the
U.S. DEPARTMENT OF ENERGY
under contract DE-AC05-84OR21400

^aOperated by Battelle Memorial Institute for the U.S. Department of Energy under contract No. DE-AC06-76RLO 1830.



7.3	STATISTICAL METHODS FOR DEVELOPING GROUT PROPERTY MODELS	39
7.3.1	Empirical-Model Forms Considered	39
7.3.2	Least-Squares Regression	44
7.3.3	Identification of Outliers and Transformations	44
7.3.4	Quality of Fit for Full and Reduced Models	45
7.3.5	Uncertainty in the Model Predictions	46
7.4	RESULTS OF MODELS FITTED TO GROUT PROPERTIES	47
7.4.1	Critical Flow Rate	47
7.4.2	10-Min Gel Strength	48
7.4.3	28-d Freestanding Liquid	49
7.4.4	Unconfined Compressive Strength	49
7.4.5	Leachability for NO ₃ + NO ₂	50
7.4.6	Adiabatic Calorimetry	51
8.	RECOMMENDED 106-AN GROUT FORMULATIONS	52
8.1	PREDICTED PROPERTIES IN THE CONSTRAINED REGION	52
8.2	RECOMMENDED GROUT FORMULATIONS FOR 106-AN	64
8.3	106-AN FORMULATIONS SELECTED	66
9.	ACKNOWLEDGMENTS	67
10.	REFERENCES	67

FIGURES

1. Schematic of the adiabatic calorimeter system	9
2. Adiabatic temperature rise of materials blended 50:50 with ground limestone and mixed at 9 lb/gal with surrogate 106-AN	22
3. Adiabatic temperature rise of attapulgite blended 30:70 with ground limestone and mixed at 6 lb/gal with surrogate 106-AN	32
4. Surface response contour plots for the critical flow rate, gallons per minute (units for the ingredients are pounds per gallon). Blacked-out regions indicate areas outside the constrained region	54
5. Surface response contour plots for the corrected unconfined compressive strength, pounds per square inch (units for the ingredients are pounds per gallon). Blacked-out regions indicate areas outside the constrained region	55
6. Surface response contour plots for the $\text{NO}_2 + \text{NO}_3$ leachability index (units for the ingredients are pounds per gallon). Blacked-out regions indicate areas outside the constrained region	56
7. Predicted critical flow rate, gallons per minute, with composition for the random grouts (units of composition are pounds per gallon)	57
8. Predicted freestanding liquid, volume percent, with composition for the random grouts (units of composition are pounds per gallon)	58
9. Predicted corrected unconfined compressive strength, pounds per square inch, with composition for the random grouts (units of composition are pounds per gallon)	59
10. Predicted $\text{NO}_2 + \text{NO}_3$ leachability index with composition for the random grouts (units of composition are pounds per gallon)	60
11. Predicted adiabatic temperature rise, °C, at 10 h, with composition for the random grouts (units of composition are pounds per gallon)	61
12. Predicted adiabatic temperature rise, °C, at 100 h, with composition for the random grouts (units of composition are pounds per gallon)	62

TABLES

1. Surrogate 106-AN composition	15
2. Phase I: Results of binder testing	18
3. Phase I: Ranking of the binders	24
4. Phase II: Results of nonbinder ingredient testing	26
5. 106-AN grout development experimental design for the smaller region only	37
6. Phase III: Results for the 106-AN mixture experiment grouts	40
7. Measured adiabatic temperature rise of 106-AN grouts, °C	42
8. Recommended grout formulations for 106-AN	64
9. Predicted properties of the recommended 106-AN grouts	65

PREFACE

This two-volume report meets the requirements for Milestone 3.4, *Final Report on Mixture-Experiment Results and Analysis*, as described in Statement of Work RDS-SOW-H-92, rev. 1, in support of the Westinghouse Hanford Grout Disposal Program. The data for this work were recorded in Laboratory notebooks A-104019-G, A-104824-G, A-104919-G, A-105040-G, and A-105093-G.

**DEVELOPMENT OF GROUT FORMULATIONS FOR 106-AN: MIXTURE-
EXPERIMENT RESULTS AND ANALYSIS**

VOL. 1. NARRATIVE AND RECOMMENDATIONS

R. D. Spence
E. W. McDaniel
Chemical Technology Division
Oak Ridge National Laboratory

C. M. Anderson
R. O. Lokken
G. F. Piepel
Pacific Northwest Laboratory*

ABSTRACT

Twenty potential ingredients were identified for use in developing a 106-AN grout formulation, and 18 were subsequently obtained and tested. Four ingredients—Type II-LA (moderate heat of hydration) Portland cement, Class F fly ash, attapulgite 150 drilling clay, and ground air-cooled blast-furnace slag (GABFS)—were selected for developing the 106-AN grout formulations. A mixture experiment was designed and conducted around the following formulation: 2.5 lb of cement per gallon, 1.2 lb of fly ash per gallon, 0.8 lb of attapulgite per gallon, and 3.5 lb of GABFS per gallon. Reduced empirical models were generated from the results of the mixture experiment. These models were used to recommend several grout formulations for 106-AN. Westinghouse Hanford Company selected one of these formulations to be verified for use with 106-AN and a backup formulation in case problems arise with the first choice.

1. INTRODUCTION

Various liquid wastes on the Hanford Reservation are being solidified/stabilized in the Grout Treatment Facility (GTF) by the Westinghouse Hanford Company (WHC). The liquid waste is mixed with cementitious or cement-based blends of dry solids in the GTF to make a fluid, pumpable slurry that is pumped to, and deposited in, a concrete vault. This cementitious product is called a grout. During FY 1991, Oak Ridge National Laboratory (ORNL) began the development of a new grout formulation for 106-AN waste in support of WHC. The purpose was (1) to develop a grout with a low heat of hydration and controlled freestanding liquid and (2) to improve its compressive strength, leach resistance, and

*Operated by Battelle Memorial Institute for the U.S. Department of Energy under contract No. DE-AC06-76RLO 1830.

durability. To meet these objectives, ORNL (1) identified potential ingredients (new and old) for this grout formulation, (2) obtained and characterized some of these potential ingredients, (3) tested the ingredients obtained, (4) selected four ingredients to use in the development, (5) conducted a mixture experiment for these four ingredients and surrogate 106-AN waste, (6) developed empirical models from the mixture experiment to predict grout performance as a function of composition, and (7) recommended grout formulations for 106-AN based on the model predictions. The development of these recommended 106-AN grout formulations is the subject of this report.

2. PROPERTY MEASUREMENTS AND REQUIREMENTS

Since the freshly mixed grout must be pumped through a few thousand feet of pipeline, the rheology and density of the freshly mixed grout are of interest. Also of interest are the freestanding liquid and heat generated as the grout solidifies in the vault and the strength, leachability, and durability of the solidified product. Thus, the rheology, density, 28-d freestanding liquid, 28-d unconfined compressive strength, nitrate plus nitrite leachability index, and susceptibility to thermal cycling were measured for the grouts mixed at ORNL, and the adiabatic calorimetry was measured for these same grouts but mixed at Battelle Pacific Northwest Laboratory (PNL).

The property requirements vary from time to time based on regulatory guidance and the changing needs of the program, but the criteria during this study follow:¹

1. critical flow rate ≤ 60 gal/min,
2. 10-min gel strength ≤ 100 lb_f/100 ft²,
3. frictional pressure drop ≤ 14 psi/100 ft,
4. freestanding liquid ≤ 0.5 vol %,
5. average 28-d unconfined compressive strength ≥ 500 psi,
6. nitrate plus nitrite leachability index ≥ 6.0 , and
7. adiabatic temperature rise $\leq 50^\circ\text{C}$.

2.1 RHEOLOGY

The rheology of the grouts was evaluated using the power-law model as the basis. The power-law model is represented by the following equation:

$$S_s = k' S_r^{n'} , \quad (1)$$

where

- S_s = shear stress, lb_f/ft^2 ;
- k' = fluid consistency index, $\text{lb}_f\text{-s}^{n'}/\text{ft}^2$;
- S_r = shear rate, s^{-1} ;
- n' = flow behavior index, dimensionless.

Shear stresses were measured on a Fann viscometer at rotor speeds of 600, 300, 200, 181, 100, 90, 60, 30, 6, 3, 1.8, and 0.9 rpm. The shear rates were obtained by multiplying the rotor speed by a constant. (The value of this constant depended on which rotor/bob combination was used; usually it was Rotor 1/Bob 1.) The two parameters, k' and n' , were estimated by plotting $\log(S_s)$ vs $\log(S_r)$, taking the least-squares regression of only the linear data points of this plot (usually the first eight rotor speeds above), and estimating k' and n' from the slope and intercept of this linear regression; thus,

$$\log(S_s) = \log(k') + n' \log(S_r) . \quad (2)$$

The slope was n' , and the intercept was $\log(k')$.

The Reynolds number for a power-law fluid is defined as²

$$N_{Re} = \frac{1.86\rho v^{(2-n')}}{k'(96/d)^{n'}} , \quad (3)$$

where

- N_{Re} = Reynolds number, dimensionless;
- ρ = grout density, lb_m/gal ;
- v = velocity, ft/s ;
- d = pipe inner diam, in.

2.1.1 Critical Flow Rate

The critical flow rate is that required to give a Reynolds number of 2100. Solving Eq. 3 for the velocity, multiplying by the cross-sectional area to give the volumetric flow rate, converting the volumetric flow rate units to gallons per minute, and substituting 2100 for the Reynolds number resulted in Eq. 4:

$$CFR = [1129k'/(96/d)^{n'}/\rho]^{1/(2-n')}\pi d^2/[(4)(0.3208)] , \quad (4)$$

where

CFR = critical flow rate, gal/min.

Summarizing, shear stress was measured as a function of shear rate for each grout using the Fann viscometer, k' and n' were estimated from these data, and the critical flow rate was calculated by substituting the k' and n' estimates into Eq. 4. (The pipe used as a basis was a 2-in. Schedule 80 pipe with an inner diam, d , of 1.939 in.) A critical flow rate of 60 gal/min, or less, was desirable.

2.1.2 Frictional Pressure Drop

The frictional pressure drop was calculated from Eq. 5:²

$$p_f = 0.039L\rho v^2 f/d , \quad (5)$$

where

- p_f = frictional pressure drop, psi;
- L = pipe length, ft;
- f = Fanning friction factor, dimensionless.

The Fanning friction factor is a function of the Reynolds number (see Fig. 11.12 in ref. 2). For laminar flow (Reynolds numbers up to 2100), the Fanning friction factor can be calculated from Eq. 6; the Reynolds number is defined by Eq. 3 for these non-Newtonian fluids:

$$f = 16/N_{Re} . \quad (6)$$

For the critical flow rate ($N_{Re} = 2100$), the Fanning friction factor is about 0.008. From Fig. 11.12 in ref. 2 for the non-Newtonian grouts, this is the lowest value of the factor for laminar flow and the highest for turbulent flow. For this project, the Fanning friction factor was assumed constant at a value of 0.008 because laminar flow was not desirable, and this was a conservative assumption for turbulent flow. By requiring flow beyond the laminar flow regime and assuming a constant friction factor, the frictional pressure drop for a given section of pipe depends only on the flow rate and density. Equation 7 gives the velocity (v) as a function of the flow rate (FR) and inner-pipe diam (d):

$$v = 0.418 \cdot FR/d^2 ,$$

where

FR = flow rate, gal/min.

Substituting Eq. 7 in Eq. 5 for v and using 100 ft, 0.008, and 1.939 in. for L , f , and d , respectively, gives Eq. 8:

$$p_f' = 0.000198\rho(FR)^2 \quad FR \geq CFR ,$$

where

p_f' = frictional pressure drop, psi/100 ft.

The critical flow rate varies with the rheology of the grouts, and, hence, the frictional pressure drop at the critical flow rate varies with rheology. It is expected, though, that the grout will be pumped at a rate of about 60 gal/min; thus, the critical flow rate should be 60 gal/min or less.¹ For the same reason, the frictional pressure drop at 60 gal/min was of more interest than that at the critical flow rate. At 60 gal/min, Eq. 8 indicates that the estimated frictional pressure drop is a function of only the grout density. This results from the requirement that 60 gal/min be beyond the laminar flow regime and the conservative

assumption of a constant value of 0.008 for the Fanning friction factor. It is preferred that the frictional pressure drop be ≤ 14 psi/100 ft. Substituting 60 gal/min and 14 psi/100 ft into Eq. 8 for FR and p_f' and solving for ρ yields

$$\rho = 19.6 \text{ lb}_m/\text{gal} ,$$

where

$$p_f' = 14 \text{ psi}/100 \text{ ft},$$

$$\text{FR} = 60 \text{ gal}/\text{min}.$$

Grout densities were in the range of 10 to 17 lb_m/gal , implying a frictional pressure drop of less than 14 psi/100 ft if the critical flow rate is less than 60 gal/min. Experience indicates that a grout of 19.6 lb_m/gal is not fluid enough for use in the GTF. In other words, if the critical flow rate is less than 60 gal/min, the frictional pressure drop will be less than 14 psi/100 ft.

2.1.3 Ten-Minute Gel Strength

The 10-min gel strength was also measured on the Fann viscometer. After measuring the grout rheology, the grout was allowed to remain static in the Fann viscometer for 10 min, the rotor was turned on at 3 rpm, and the maximum Fann viscometer reading was noted and recorded. This reading is the 10-min gel strength in units of $\text{lb}_f/100 \text{ ft}^2$. A 10-min gel strength of 100 $\text{lb}_f/100 \text{ ft}^2$ or less is desired.

2.2 GROUT DENSITY

The density of the freshly mixed grout was measured using a Baroid mud balance. The solids tended to settle in the quiescent grouts, leading to freestanding liquid over a solid monolith. In general, this monolith was denser than the overall density measured with the mud balance. Some of the freestanding liquid was reabsorbed as the grout cured, but the monolith volume was dictated by this early settling (i.e., any volume changes after the grout sets were minor). The Baroid balance was designed to eliminate air and to weigh a set volume of grout. Most grouts were fluid and easily released air bubbles. Thicker grouts and

air-entraining admixtures tended to retain more of this air. The measured density was an overall density (including grout, free liquid, and air), and affecting the air retention made the measured densities more variable.

2.3 FREESTANDING LIQUID

Approximately 250 mL of the freshly mixed grout was poured into a tared 500-mL polyethylene bottle, sealed with a screw-on polyethylene lid, weighed, and placed into an oven maintained at 40°C. The solids were allowed to settle, forming a freestanding liquid above the grout. The freestanding liquid was measured after mixing at times of 2 h, 1 d, 2 d, 7 d, 14 d, 21 d, and 28 d.

The procedure for this measurement was as follows: (1) weigh the bottle before opening; (2) open, pipette off the freestanding liquid, and weigh this liquid; (3) weigh the bottle containing the remaining grout; and (4) replace the freestanding liquid, reseal the bottle, and replace it in the oven. (This gave an independent weight of the total of grout and liquid prior to unsealing at each time period so that losses from evaporation and handling could be monitored.) A conservative estimate of the freestanding liquid was obtained by totaling the measured mass of freestanding liquid and the mass loss (i.e., the difference between the initial total mass and the sum of the grout and liquid masses). The volume of freestanding liquid was estimated by dividing this conservative mass estimate of the freestanding liquid by the density of the surrogate 106-AN at 40°C (1.21 g/mL). The original grout volume was estimated by dividing the initial grout mass by the measured grout density. The volume percent of freestanding liquid was calculated by dividing the estimated volume of liquid by the estimated original volume of grout and multiplying by 100. (Evaporative losses were only a few tenths of volume percent. Handling losses were about the same but more variable and could range higher. Thus, reported freestanding liquid of only a few tenths of a volume percent usually meant that no liquid was actually observed, and the reported value reflects the mass loss during the test.) The preferred freestanding liquid depends on a developing process strategy. The experimental work was performed based on a criteria for freestanding liquid of 0.5 vol % or less from the criteria document.¹ Since process strategy requires evaporative cooling, some of the postexperimental analysis used a value of 3.0 vol % or less for grout recommendation.

2.4 ADIABATIC CALORIMETRY

The adiabatic calorimeter system used in these studies consists of eight individual calorimeter cells and a common temperature measurement and control system. Figure 1 shows a schematic of a cell. The calorimeter cells consist of a 6-L stainless steel (SS) Dewar, a water circulation pump, an immersion heater, and a 1-L SS Dewar for the grout slurry. The heater is controlled with a solid-state relay connected to the control system. The data acquisition system consists of a relay multiplexer, a thermocouple amplifier/conditioner, and a 16-bit analog-to-digital converter.

Adiabatic calorimetry testing of grout hydration is based on the premise that all the heat generated by the grout is retained within the grout, which increases the grout temperature. For the large grout disposal vaults, near adiabatic curing conditions are expected, particularly near the center of the vault. In the laboratory adiabatic conditions are achieved by placing freshly prepared grout slurry into an SS Dewar. A thermocouple is then inserted into the grout slurry. The Dewar containing the grout slurry is then placed into a second, larger Dewar containing water preheated to the initial grout temperature. A heater in the larger Dewar maintains the temperature of the water bath at the same temperature as the grout. In an ideal system no heat transfer between the grout and the surroundings can occur because the temperatures within the grout and the water are the same at all times.

The adiabatic calorimetry was measured at PNL; the other properties listed in this report were measured at ORNL. While all of the measurements for a given batch at ORNL were for the same dry solids blend and grout mix, the adiabatic calorimetry was performed on samples blended and mixed at PNL. The dry solids were from the same sources and were blended in the same proportions. The surrogate waste was prepared identically, and the grouts were mixed at identical mix ratios; so, ostensibly the adiabatic calorimetry measured was representative of the grouts tested at ORNL. Because PNL blended and mixed separate batches of the grouts for the calorimetry, the blending and mixing procedures at PNL are included in this subsection. The only difference noted was the temperature of the surrogate waste prior to mixing the grouts. The surrogate was heated to 40°C at ORNL and to 45°C at PNL.

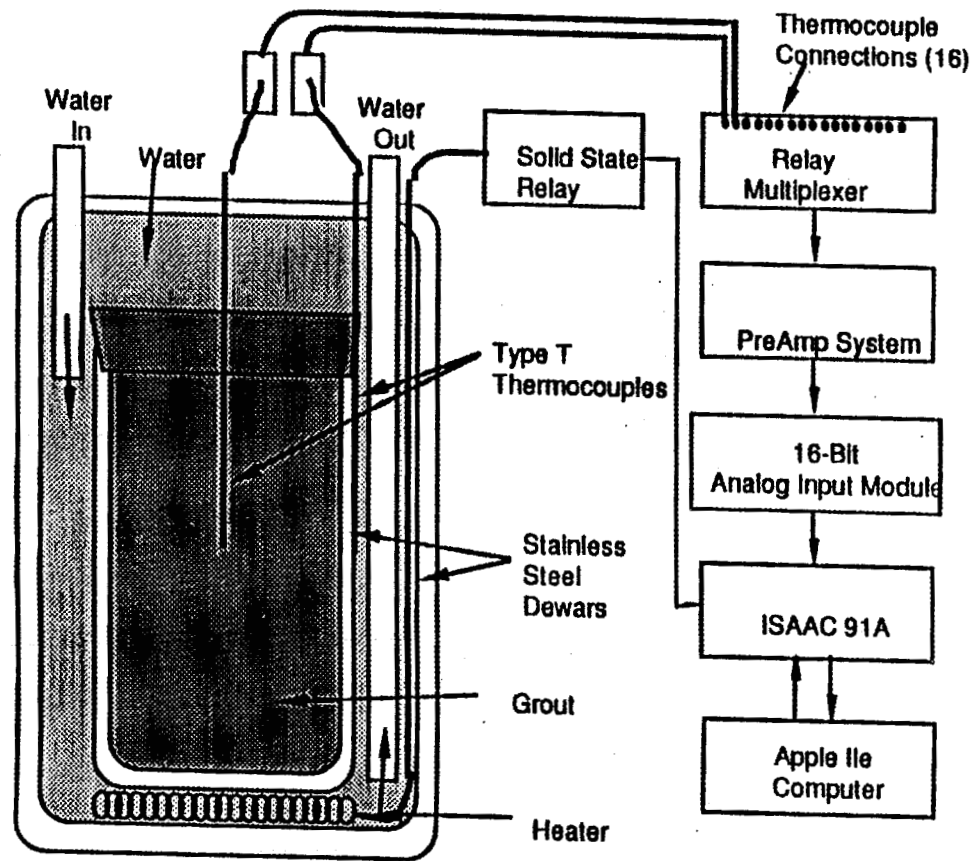


Fig. 1. Schematic of the adiabatic calorimeter system.

2.4.1 Dry Blend

When dry blending was performed, a V-blender was used for 23 h. No dry blending was performed during Phase I because it tested only individual dry materials, the binders, with the surrogate 106-AN. Several two-material blends were made during Phase II, Type II-LA (moderate heat of hydration) Portland cement with one of eight candidate dry materials. The candidate dry materials tested during Phase II consisted of Class F fly ash, ground limestone, ground air-cooled blast furnace slag (GABFS), air-cooled blast furnace slag (ABFS) aggregate, sand, attapulgite clay, sodium silicate powder, and slaked lime. The individual materials of the dry blend for Phase III included Type II-LA (moderate heat of hydration) Portland cement from Ash Grove Cement West; Class F fly ash from Centralia, Washington; attapulgite clay from Engelhard Corporation; and GABFS obtained from C. T. Takahashi Company.

2.4.2 Grout Preparation

Grout slurries were prepared using a Hobart mixer and a wire whip. Simulated 106-AN waste (1-L) was preheated to approximately 45°C and placed in the mixer. Room temperature dry blend was added while the mixer was running. After 1 min of total mixing (i.e., 30 s on low and 30 s on high), approximately 1 L of grout slurry was poured into an SS Dewar, which was placed into a calorimeter cell.

2.5 28-d UNCONFINED COMPRESSIVE STRENGTH

The freshly mixed grout was poured into 2-in.-cube molds, which were placed in a humidity cabinet at 40°C and >95% relative humidity. The next day the mold was moved to a humidity cabinet at 90°C and >95% relative humidity, and the grout was allowed to cure for another 27 d (a total of 28 d) at these conditions. The cubes were removed from the mold during the 28-d cure and returned to the cabinet inside plastic bags after the grout had set (or solidified). On the 28th d after mixing, the unconfined compressive strength of the cubes was tested on a Tinius Olsen Super L Universal Testing Machine. This device measures the force required to crush the cube. This force was divided by the measured area to obtain the true compressive strength (pounds per square inch) of the solid sample. The separation of the freestanding liquid typically gave a cube side of less than 2×2 in. (4 in.²)

(a side of the cubes was crushed rather than the top or bottom). This unconfined compressive strength was corrected to the originally poured 2-in. cube by dividing the crushing force (lb_f) by 4 in.^2 to give a conservative corrected 28-d unconfined compressive strength. A mean unconfined compressive strength of 500 psi was preferred.¹

2.6 NITRATE AND NITRITE LEACHABILITY

The freshly mixed grout was poured into cylindrical molds (2.5-cm diam \times 4.65-cm high). The molds were placed in a humidity cabinet at 40°C and >95% relative humidity. The next day the molds were moved to a humidity cabinet at 90°C and >95% relative humidity for another 27 d (a total of 28 d). The samples were removed from the molds after set (or solidification) and placed inside plastic bags inside the humidity cabinet. After 28 d the samples were leached according to the ANSI/ANS-16.1-1986 5-d leach procedure. The leachant was house-distilled water distilled again in a quartz still (i.e., double-distilled water with second distilling in a quartz still). The leachant was changed at leaching times of 2 h, 7 h, 1 d, 2 d, 3 d, 4 d, and 5 d in addition to a 30-s rinse prior to the start of leaching. (A few milliliters of boric acid solution were added to each leachate to preserve the nitrate against biological consumption.) The freestanding liquid was preserved and added to the rinse. The nitrate and nitrite concentrations of the leachates were measured using a Wescan ion chromatograph. The effective diffusion coefficient of nitrate plus nitrite was estimated by mathematically adding the rinse inventory to the first leach interval and forcing the diffusion portion of the model through the origin. This approach skews the model from the data points but combines the diffusion-control leaching and instantaneous release into a single parameter for comparative purposes. The leachability index was defined as the negative logarithm of the effective diffusion coefficient. Higher leachability indexes are desired, preferably greater than 6.

2.7 THERMAL CYCLING

Nuclear Regulatory Commission guidance made it possible that thermal cycling of the waste forms would be required. Because thermal cycling required little effort, it was routinely included in the suite of tests. Later guidance makes it clear that this grouting will not be exposed to thermal cycling, but since thermal cycling was performed, the results are reported.

Cubes cured in the same manner as the 28-d unconfined compressive strength samples were subjected to thermal cycling (after curing 28 d). Comparative cubes were placed in a humidity cabinet at room temperature and >95% relative humidity so that the unconfined compressive strength on samples as old as the cycled samples could be used for comparison as well as the 28-d unconfined compressive strength. Bare cubes were cycled between 60 and -40°C for 30 cycles. The samples were placed in the environmental chamber while it was at 25°C prior to increasing to 60°C . One cycle of the environmental-chamber temperature was ramp in about 1 h from 25 to 60°C , hold at 60°C for 1 h, ramp in about 1 h from 60 to 25°C , hold at 25°C for 1 h, ramp in about 1 h from 25 to -40°C , hold at -40°C for 1 h, ramp in about 1 h from -40 to 25°C , hold at 25°C for 1 h, and start again. After 30 cycles, the unconfined compressive strength of the cycled samples and the comparative samples were measured. Once again, the correction for the volume loss from freestanding liquid was made by assuming perfect 2-in. cubes in calculating the pounds per square inch.

3. MATERIALS

Twenty potential ingredients—Type II-LA Portland cement, GGBFS, Type IV Portland cement, Type V Portland cement, Class H cement, fluidized-bed combustor ash, Class F fly ash, ground limestone, GABFS, ABFS aggregate, sand, attapulgite clay, sodium silicate powder, slaked lime, and six liquid admixtures—were identified for use in developing a 106-AN grout formulation. Samples were obtained and tested for all except Type IV Portland cement and fluidized-bed combustor ash. Type IV Portland cement is produced only for large guaranteed markets (e.g., constructing a dam). Fluidized-bed combustor ash, like Class F fly ash, is a waste by-product of energy production but, unlike Class F fly ash, is not currently marketed.

Five of the dry-solids candidates—Type II-LA Portland cement, Type V Portland cement, Class H cement, GGBFS, and activated Class F fly ash—that were obtained were potential binders. The nonbinder candidates were selected to modify grout properties or to alleviate known problems with 106-AN grout formulations. Two dry-solids candidates—attapulgite clay and sodium silicate—were primarily included because of their known ability to control freestanding liquid. Four dry-solids candidates—ground limestone, GABFS, ABFS aggregate, and sand—were primarily included as inert fillers to keep the solids content high without increasing the heat evolution. GABFS was obtained from two

sources: Takahashi and Standard Slag. The slaked lime was included primarily to precipitate phosphate in the 106-AN. The phosphate had the potential of retarding set and allowing more time for solids to settle, which indirectly increased the freestanding liquid. Slaked lime in this report means a dry powder of calcium hydroxide to be blended with the other dry powders prior to mixing with surrogate 106-AN.

Class F fly ash was the only candidate tested as both a potential binder and as a nonbinder ingredient. Usually, Class F fly ash is used as a pozzolan in combination with cement, but it can be activated with sodium hydroxide to solidify. Because 106-AN has a high sodium hydroxide concentration, Class F fly ash was tested as the potential binder without the more exothermic cements and granulated slags in an attempt to develop a formulation with extremely low-heat evolution. Unfortunately, the Class F fly ash was not an effective binder alone, as demonstrated later in this report. It was still tested as a pozzolan additive. Pozzolans interact with cements to make a stronger, less porous product. In other words, the fly ash can replace some of the cement without sacrificing strength and lead to lower-heat evolution. Strictly speaking, the fly ash was not truly a “nonbinder,” but for the purposes of this report, the cements and granulated slags were defined as “binders,” and the pozzolan fly ash was defined as one of the “nonbinder ingredients.”

The six admixtures were a fluidizer, a set modifier, and an air entrainer for two vendors. Sika supplied the Sikament 300, the Plastiment, and the Sika AEA-15; Masterbuilders supplied the Rheo-Build 716, the Delvo stabilizer, and the Micro-Air, respectively, for a fluidizer, a set modifier, and an air entrainer. The intent was to obtain the preferred grout properties with dry-solids ingredients and not to use admixtures unless necessary but also to verify the effectiveness of admixtures with 106-AN grouts.

Fluidizers are used to make grouts less viscous and can be used to increase the solids content while holding the Reynold's number constant. This results in less freestanding liquid for a grout with essentially the same rheology.

Set modifiers can be used to accelerate or retard grout set. If the rate of set could be matched with the rate of heat loss from the vault, a possible means was available to limit vault temperatures to 90°C. Obviously, this could be a risky approach, if it could be done at all, in that months might be required to dump the heat generated while assuring regulators that the grout will eventually set into a solid product. Some set retarders were advertised to be able to stop hydration completely for days, maybe weeks.

Air entrainers help retain small air bubbles in the grout through its fluid period until set traps the bubbles in the grout. The bubbles help protect the grout from freeze/thaw damage,

making the product more durable. In general, these admixtures had the expected effects and are available in the future if the need arises.

Phase I tested the five potential binders: Type II-LA Portland cement, GGBFS, Type V Portland cement, Class H cement, and activated Class F fly ash. Phase II tested 12 potential ingredients with one binder, Type II-LA Portland cement, and selected four ingredients: Type II-LA Portland cement, Class F fly ash, attapulgitic clay, and GABFS. Phase III conducted a mixture experiment using these four ingredients mixed with surrogate 106-AN to develop recommended 106-AN grout formulations.

Both GGBFS and GABFS are ground blast furnace slags, but GGBFS is granulated or water-quenched slag, and GABFS is air-cooled slag. GGBFS is glassy and can be activated to react and form cementitious products. GABFS is crystalline and virtually nonreactive in the cementitious environment. Thus, GGBFS is an excellent binder and forms a leach-resistant waste form, while GABFS is just a nonreactive filler.

4. SAMPLE PREPARATION PROCEDURES

4.1 BLENDING

Dry materials were blended for 23 h in a 3-ft³ Patterson-Kelley twin-shell V-blender in enough quantity to make three batches of grout. (Single dry ingredients were not blended.)

4.2 MIXING

The surrogate 106-AN was made in batches of 20 L to the composition listed in Table 1. The surrogate was heated to 40°C, and the desired volume was added to the mixing bowl of a Model N-50 Hobart mixer. The dry blend was added to this liquid over about 15 s while mixing with the wire whisk on low speed (~140 rpm) and was then mixed an additional 15 s at this speed (a total of 30 s mixing on low). The speed was then set to medium (~285 rpm), and the grout was mixed for an additional 30 s at this speed (a total mixing time of 60 s). The freshly mixed grout was then tested and poured (or spooned) into molds. Each grout was mixed in three separate batches. The following tests and samples were conducted and prepared for each batch:

Table 1. Surrogate 106-AN composition

Component	Molarity
NaAl(OH) ₄	0.421
Na ₂ SO ₄	0.031
NaCl	0.15
NaF	0.0081
Ca(NO ₃) ₂ · 4H ₂ O	0.002
NaOH	0.675
NaNO ₃	1.29
NaNO ₂	0.758
Na ₂ CO ₃	0.382
HEDTA	0.019
Na ₄ EDTA	0.0044
Glycolic acid	0.042
Na ₃ PO ₄ · 12H ₂ O	0.155
Na ₃ C ₆ H ₅ O ₇ · 2H ₂ O	0.03
<i>Ionic</i>	
Na ⁺	4.70
OH ⁻	2.36
NO ₃ ⁻	1.33
NO ₂ ⁻	0.758
Al ³⁺	0.421
CO ₃ ²⁻	0.382
PO ₄ ³⁻	0.155
Cl ⁻	0.150
SO ₄ ²⁻	0.031
C ₆ H ₅ O ₇ ³⁻	0.030
F ⁻	0.0081
Ca ²⁺	0.0020

1. rheology,
2. density,
3. one freestanding liquid sample,
4. three 2-in. cubes, and
5. three leach-cylinder samples.

This gave three independent measurements of the rheology, density, and freestanding liquid, nine 2-in. cubes for unconfined compressive strength and thermal cycle testing, and nine cylinders for leaching. One cube from each batch was tested for 28-d unconfined compressive strength. Another cube from each batch was subjected to thermal cycle testing. The remaining cubes were used as comparator cubes in thermal cycling. (Sometimes not all nine cubes survived curing, in which case three comparator cubes were not available.) Only three cylinders—one from each batch—were subjected to leach testing.

5. PHASE I: BINDER TESTING

It was desired to perform a mixture experiment on three or four ingredients for the 106-AN grout development.³ It was necessary to select these three or four ingredients out of the 18 obtained and tested. To achieve these aims, the experimental design was divided into three phases: Phase I to test the binders, Phase II to test the other ingredients, and Phase III to select ingredients and perform a mixture experiment.³ This section reports on Phase I; Sects. 6 and 7 report on Phases II and III respectively.

5.1 EXPERIMENTAL TEST-PLAN DESIGN

Five potential binders—Type II-LA Portland cement, GGBFS, Type V Portland cement, Class H cement, and activated Class F fly ash—were tested in Phase I. Class F fly ash alone (i.e., fly ash is usually used in combination with lime or cement) is not a standard binder, but sodium hydroxide is known to activate Class F fly ash into solidifying. Because 106-AN contains a significant concentration of sodium hydroxide, the binding capability of Class F fly ash was tested alone. A minimum binder mix ratio of about 2 lb/gal is needed to form a solid product, and the Fann viscometer can handle a maximum mix ratio of about 15 lb/gal. A single binder was considered sufficient for this application; so interactions were ignored.

Each binder was tested at 2 and 15 lb/gal (a total of 10 grouts). A minimum of five grouts was needed for the first-degree empirical model for comparing the binders.

5.2 RESULTS

Table 2 summarizes the Phase I results for critical flow rate, 10-min gel strength, 28-d freestanding liquid, corrected 28-d unconfined compressive strength, and thermal cycling. Phase I was a mixture experiment conducted on only the binders mixed with surrogate 106-AN and constrained to the vertices at a high- and low-mix ratio of 2 and 15 lb/gal. The purpose was to select one binder to use in developing the 106-AN grout formulations; hence, binder interactions were not tested. Empirical first-degree polynomial models were generated by multiple linear regression of the data in Table 3 using Lotus^R 1-2-3. These models are presented in the following equations; the estimated standard deviations of the coefficients are given in parentheses below the coefficient. The multiple correlation coefficients (R^2) and estimated root mean squared error (RMSE) of the grout property data calculated by Lotus^R 1-2-3 are given below each equation.

$$\text{CFR} = -3.2 + 3.5 W_1 + 2.1 W_2 + 14.1 W_5 + 4.0 W_6 + 2.2 W_7 \quad (10)$$

(0.4) (0.4) (0.4) (0.4) (0.4)

$$R^2 = 0.98$$

$$\text{RMSE} = 8.2 \text{ gal/min}$$

$$\text{GS} = -2.5 + 2.6 W_1 + 0.67 W_2 + 2.5 W_5 + 2.2 W_6 + 1.2 W_7 \quad (11)$$

(0.1) (0.09) (0.1) (0.2) (0.1)

$$R^2 = 0.98$$

$$\text{RMSE} = 2.1 \text{ lb}_f/100 \text{ ft}^2$$

$$\text{FSL} = 76 - 5.1 W_1 - 4.8 W_2 - 5.1 W_5 - 5.1 W_6 - 4.1 W_7 \quad (12)$$

(0.2) (0.2) (0.2) (0.2) (0.2)

$$R^2 = 0.98$$

$$\text{RMSE} = 4.6 \text{ vol \%}$$

$$\text{UCS} = -315 + 255 W_1 + 68 W_2 + 387 W_5 + 306 W_6 + 210 W_7 \quad (13)$$

(14) (14) (14) (14) (14)

$$R^2 = 0.98$$

$$\text{RMSE} = 316 \text{ psi}$$

Table 2. Phase I: Results of binder testing

Mix ratio	CFR ^b	GS ^c	FSL ^d	Corrected UCS ^e		
				28 d ^e	TC ^f	C ^g
<i>Type II-LA Portland cement</i>						
2 lb/gal	5	1.5	62.	133	128	104
	6	1.	63.	155	155	196
	5	1.5	62.	114	56	113
15 lb/gal	51	37.	0.13	3520	4168	4268
	49	36.	0.09	3258	3953	3685
	49	36.5	0.10	3780	4247	3928
<i>Ground granulated blast furnace slag</i>						
2 lb/gal	7	1.	63.	119	327	136
	7	1.	60.	98	266	138
	7	1.	60.	98	249	95
15 lb/gal			0.43	4998	2848	4653
	222	31.	0.40	6118	5510	4455
	201	41.	0.15	5478	5295	5610
<i>Class F fly ash</i>						
2 lb/gal	7	1.6	69.	402	238	
	8	1.5	67.	421	527	312
	9	1.3	69.	396		
15 lb/gal	28	7.5	2.2	540	912	618
	27	7.	2.9	648	870	714
	27	7.	3.8	686	863	583
<i>Type V Portland cement</i>						
2 lb/gal	5	1.	63.	104	268	106
	9	1.2	63.	169	284	91
	10	1.2	60.	147	248	174
15 lb/gal	57	34.	0.13	4435	4295	4130
	58	30.	0.53	4148	4413	3985
	55	29.5	0.13	4320	4580	4255

Table 2 (continued)

Mix ratio	CFR ^b	GS ^c	FSL ^d	Corrected UCS ^a		
				28 d ^e	TC ^f	C ^g
<i>Class H cement</i>						
2 lb/gal	6	1.	72.	103	89	77
	8	1.	76.	126		134
	8	1.	83.	47	54	33
15 lb/gal	29	16.	14.	2853	3280	2923
	28	16.5	12.	2993	2925	2935
	29	15.	11.	2663	2773	2585

^aUnconfined compressive strength corrected to a 2-in. cube, psi.

^bCritical flow rate, gal/min.

^c10-min gel strength, lb_f/100 ft².

^d28-d freestanding liquid, vol %.

^eAfter curing 28 d.

^fAfter thermal cycling.

^gComparator sample, same age as thermal cycled sample but not subjected to thermal cycling.

$$TC/C = 1.86 - 0.06 W_1 - 0.03 W_2 - 0.06 W_5 - 0.05 W_6 - 0.06 W_7 \quad (14)$$

$$(0.03) (0.03) (0.03) (0.03) (0.03)$$

$$R^2 = 0.31$$

$$RMSE = 0.58$$

where

CFR = critical flow rate, gal/min;

GS = 10-min gel strength, lb_f/100 ft²;

FSL = 28-d freestanding liquid, vol %;

UCS = corrected 28-d unconfined compressive strength, psi;

TC/C = ratio of the corrected unconfined compressive strengths of the thermally cycled sample to the comparator sample;

W₅ = mix ratio of GGBFS, lb/gal;

W₆ = mix ratio of Type V Portland cement, lb/gal;

W₇ = mix ratio of Class H cement, lb/gal;

R² = multiple correlation coefficient.

These first-degree models were used to compare the binders qualitatively and were not intended as a tool for accurate prediction of grout properties. All of the correlation coefficients, except for TC/C, were close to one, giving confidence that these equations accurately reproduce the observed values. The observed TC/C values were scattered in a fairly narrow band around a value of one (more values were above one than below). Apparently, the change in this value with compositional changes cannot be distinguished significantly from the variability in replicates for this ratio. In other words, the low correlation coefficient indicates that correlation of TC/C with composition cannot be found with confidence for this data set.

The effect of each binder on a given property can be ranked qualitatively and quantitatively by comparing the values of the estimated coefficients. Equation 10 illustrates that the ranking from best to worst was (1) fly ash and Class H cement (about equal ranking), (3) Type II Portland cement, (4) Type V Portland cement, and (5) GGBFS regarding to the critical flow rate. Quantitatively, the coefficient for GGBFS was far different than the other four coefficients, implying a totally different level of performance for GGBFS compared with the other four binders.

Similarly, for 10-min gel strength, Eq. 11 illustrates a ranking of (1) fly ash, (2) Class H cement, and (3) Type V Portland cement, GGBFS, and Type II Portland cement (the last three were of about equal ranking). For 28-d freestanding liquid, Eq. 12 illustrates a ranking of (1) Type II Portland cement, GGBFS, and Type V Portland cement (these three were of about equal ranking), (4) fly ash, and (5) Class H cement. And for 28-d corrected unconfined compressive strength, Eq. 13 illustrates a ranking of (1) GGBFS, (2) Type V Portland cement, (3) Type II Portland cement, (4) Class H cement, and (5) fly ash.

Correlation for Eq. 14 was poor, and the rankings were inconclusive. TC/C was the ratio of the unconfined compressive strength of the sample subjected to thermal cycling to the unconfined compressive strength of the comparator sample of the same age but not subjected to thermal cycling. It was intended to be a measure of the durability of the grouts. The results proved that these grouts survived thermal cycling intact with close to the same compressive strength and a tendency toward an improved compressive strength. It is not clear why the thermally cycled samples were stronger. Perhaps using bare samples led to evaporation of all unbound water, precipitation of salt in the grout pore structure, and the solid salt added to the grout strength. The data hints that GGBFS had even more of a tendency to increase in strength with thermal cycling than the four other binders, but the

effect was too small and the data scatter was too large to be conclusive. One can conclude that thermal cycling will not weaken these binders.

Although adiabatic calorimetry was only routinely measured for the mixture experiment grouts of Phase III, the adiabatic calorimetry of six of the ingredients—Type II-LA Portland cement, Class F fly ash, GGBFS, Type V Portland cement, and GABFS—were measured individually in combination with another additive, ground limestone. These seven ingredients include four out of five of the binders tested in Phase I (i.e., Class H cement was the binder not tested) and the binder (i.e., Type II-LA Portland cement) and three of the additives (i.e., ground limestone, GABFS and attapulgite clay) tested in Phase II. All, except for the attapulgite clay, were blended in equal proportions with ground limestone and mixed with surrogate 106-AN at a total mix ratio of 9 lb/gal at 40°C, giving five grouts composed of 4.5 lb of the ingredient being tested per gallon and 4.5 lb of ground limestone per gallon. Previous calorimetry had demonstrated no measured temperature rise for the ground limestone (at 9 lb/gal); thus, the measurements gave the heat evolution of these ingredients (at 4.5 lb/gal) presented as the temperature rise for the grouts at 9 lb/gal. Figure 2 illustrates the measured temperature profiles for these grouts. Because ground limestone did not contribute any heat evolution, the profile for ground limestone would have simply been a horizontal line at 40°C in Fig. 2. The adiabatic calorimetry of the ground limestone, the GABFS, and the attapulgite are discussed in Subsect. 6.2.

The two cements gave profiles typical of initially high exothermic reaction rates that rapidly declined as the reactants were exhausted; the Type V profile was significantly higher than that of Type II. The Type V profile apparently had a higher heat of hydration, since it appeared to be approaching a higher final temperature than did the Type II profile. The Class H cement can be speculated to have given a profile similar to these two cements. The temperature profile of the Class H cement was not measured, but it can be assumed that the final temperature approached would have been in the same range as the two cements measured. Although the rate of approach will be important during processing or for modeling, the final adiabatic temperature (or maximum adiabatic temperature) was the basis for ranking in this report, meaning the Type II-LA (moderate heat of hydration) Portland cement ranked ahead of the Type V Portland cement. The Class H temperature profile was not measured, but Class H cement should be ranked equal with the Type II-LA (moderate heat of hydration) Portland cement because lower heats of hydration may be specified for Class H cements.

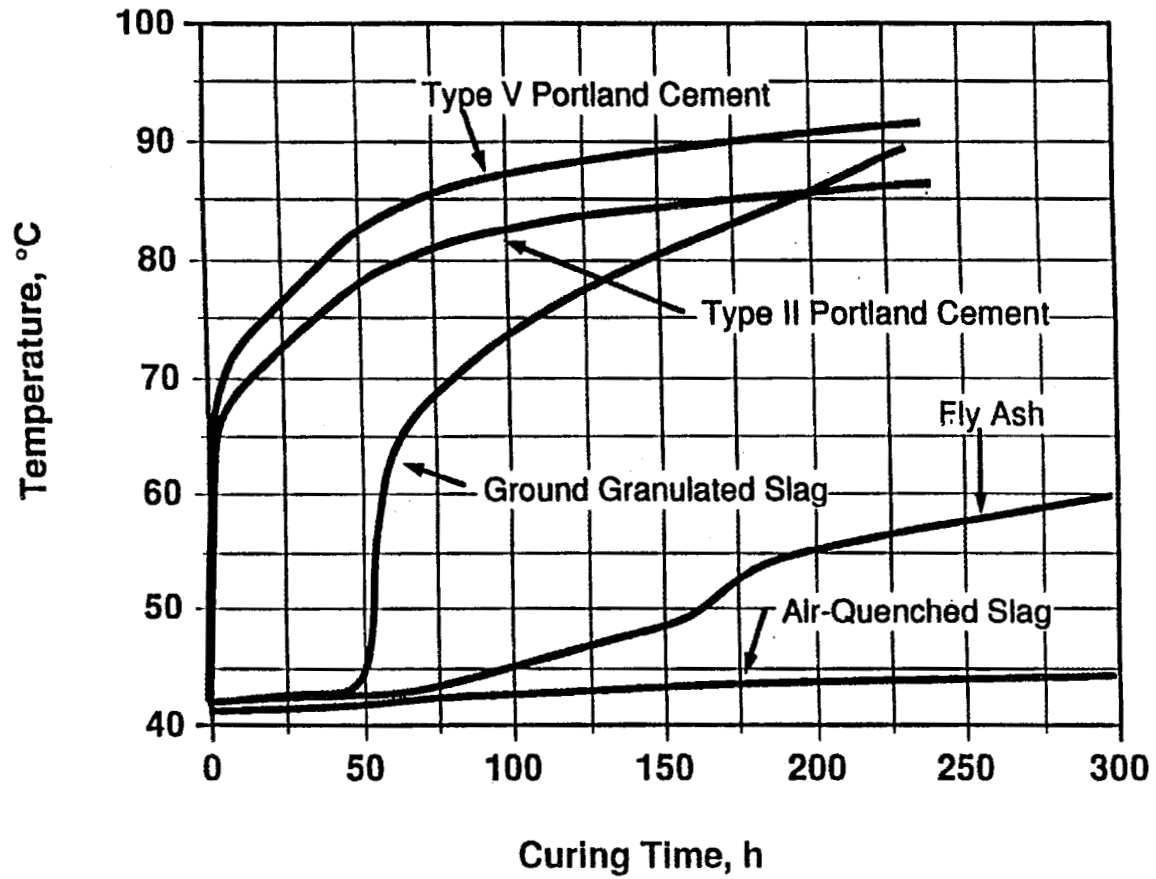


Fig. 2. Adiabatic temperature rise of materials blended 50:50 with ground limestone and mixed at 9 lb/gal with surrogate 106-AN.

The other measured temperature profiles were more complicated than the simple profiles for the cements. The GGBFS had little or no increase for several hours, followed by an exponential increase similar to the cement profiles. This behavior was interpreted as a delayed cementitious reaction and is typical for the glassy slags. GGBFS must be activated by a base that dissolves the glassy material prior to reaction. This delay in the onset of reaction complicates the processing steps and the performance of GGBFS grouts. One objective of processing is to fill the vaults in a series of lifts to allow removal of as much heat as possible before forming the final giant monolith. The delayed onset of reaction for GGBFS would work counter to this strategy. Also, delaying set for so long allows the maximum time and maximum fluidity for solids settling, leading to increased freestanding liquid. In addition, the projected profile for GGBFS leads to a final higher adiabatic temperature than for any of the other materials, including the Type V Portland cement. This observation was consistent with the well-known fact that GGBFS has a higher heat of hydration than Portland cements. For these reasons, GGBFS has the lowest ranking for adiabatic calorimetry of the five binders tested.

Fly ash is also glassy; hence, it was not surprising that it also had a delay in accelerated temperature rise. Although the shape of the fly-ash curve in Fig. 2 shows little or no decrease in the rate of rise after about 190 h, the final temperature is still expected to be well below that of the cements and GGBFS. This expectation gives fly ash the highest ranking among the binders when only the maximum adiabatic temperature is used from the adiabatic calorimetry.

In summary, the ranking of the heat evolution of the binders is (1) Class F fly ash, (2) Type II-LA (moderate heat of hydration) Portland cement and Class H (low heat of hydration) cement (about equal ranking), (4) Type V Portland cement, and (5) GGBFS. Table 3 summarizes the rankings of the five binders for each of the measured properties. Type II cement and fly ash had the best average ranking among these five binders, followed by Type V Portland cement and Class H cement. GGBFS had the worst average ranking of these five binders. The fly ash had problems with freestanding liquid and low compressive strengths. The data indicated that the old preferred compressive strength of >60 psi was achievable with activated Class F fly ash as the binder but that the new preferred value of >500 psi probably was not. In other words, fly ash alone will not make a strong product and was not acceptable as the binder. Thus, Type II-LA (moderate heat of hydration) Portland cement was selected as the binder of choice for developing the 106-AN grout formulation.

Table 3. Phase I: Ranking of the binders

Property	Binder ^a				
	Type II-LA Portland cement	Activated Class F fly ash	Ground granulated blast furnace slag	Type V Portland cement	Class H cement
Critical flow rate	3	1	5	4	1
10-min gel strength	3	1	3	3	2
28-d free-standing liquid	1	4	1	1	5
28-d unconfined compressive strength	3	5	1	2	4
Thermal cycling durability	1	1	1	1	1
Heat evolution	2	1	5	4	2
Average	2.2	2.2	2.7	2.5	2.5

^aHighest = 1; lowest = 5.

One property not included in Table 3 was leachability. GGBFS was expected to have an advantage in leach resistance, especially in retaining technetium. The high freestanding liquids of fly ash and Class H cement were expected to put these two potential binders at a disadvantage in leach resistance. In other words, less leach resistance was expected by using Type II cement as the binder rather than GGBFS. This was not considered a serious disadvantage since all of the binders were expected to achieve the preferred leachability index of >6.0.

6. PHASE II: INGREDIENT SELECTION

6.1 EXPERIMENTAL TEST-PLAN DESIGN

The remainder of the ingredients were tested with the Type II-LA Portland cement as a binder. Six of the dry-solids additives (i.e., Class F fly ash, ground limestone, GABFS, attapulgite clay, sodium silicate powder, and slaked lime) were tried at mix ratios of 2 and 13 lb/gal of cement and additive respectively (a total mix ratio of 15 lb/gal). Two of the dry-solids additives (i.e., sand and ABFS aggregate) were not tested because the materials were too coarse to mix properly using the laboratory mixing procedure. The coarse sand and aggregate immediately segregated at the bottom of the grout mixes. This was considered sufficient grounds for rejecting these materials because the fluid grouts required for the Grout Processing Facility would likely have had problems handling these coarse materials.

The liquid admixtures were tested in combination for each vendor (i.e., 5 wt % for each admixture for a total of 15 wt % for the grout tested for each vendor). (Liquid admixtures will not be used unless the desired properties cannot be obtained with the other ingredients.) The liquid admixtures were added to the liquid waste, and this combination was tested at two mix ratios: 2 and 15 lb/gal of Type II-LA Portland cement.

Not all of these grouts could be tested. Adjustments were made for some of these ingredients. The results allowed comparison of those ingredients tested.

6.2 RESULTS

Table 4 summarizes the Phase II results for the critical flow rate, 10-min gel strength, 28-d freestanding liquid, corrected 28-d unconfined compressive strength, and thermal cycling. Phase II was an attempted mixture experiment to test potential additives with the selected binder (i.e., Type II-LA Portland cement) and surrogate 106-AN. The mixes were constrained to the vertices at high- and low-mix ratios of the additives and the binder. Unlike the binder, no minimum was required for the additives, and the Phase I results at 2 and 15 lb/gal Type II-LA Portland cement were used as the vertices for low additive content (i.e., 0 lb of additive per gal). The other vertices were determined by constraining the total mix ratio to ≤ 15 lb/gal and the binder mix ratio to ≥ 2 lb of binder per gal. Thus, most of the new grouts for Phase II consisted of mix ratios of 2 lb of binder per gal and 13 lb of

Table 4. Phase II: Results of nonbinder ingredient testing

Mix ratio (lb/gal)		CFR ^a	GS ^b	FSL ^c	Corrected UCS ^d		
Ingredient	Cement				28 d ^e	TC ^f	C ^g
<i>Class F fly ash, Type II-LA Portland cement</i>							
13.	2.	30	12.5	0.16	3635	3085	3170
		31	11.5	0.19	3648	2733	3353
		32	12.5	0.36	3215	2708	3383
<i>Attapulgate clay, Type II-LA Portland cement</i>							
1.73	0.27	34	14.5	28.	4	7	5
		32	12.	30.	2	3	4
		33	12.5	29.	2		4
2.	13.	169	104.5	0.03	2463	3075	2735
		168	195.	0.03	2930	3078	2633
		166	128.	0.03	2793	3120	2680
<i>Standard Slag GABFS, Type II-LA Portland cement</i>							
13.	2.	40	22.5	1.7	246	461	251
		39	19.5	1.5	222	454	252
		40	20.	2.9	257	318	259
<i>Takahashi GABFS, Type II-LA Portland cement</i>							
13.	2.	53	25.5	0.23	367	387	393
		52	27.5	0.4	371	425	
		51	26.5	0.4	354	377	388
<i>Ground limestone, Type II-LA Portland cement</i>							
13.	2.	41	18.5	6.2	95	327	84
		42	19.5	6.3	94	330	90
		42	19.5	5.0	98	316	93
<i>Sodium silicate, Type II-LA Portland cement</i>							
13.	2.	161	22.5	0.10	0		
		159	25.	0.07	0		
		164	35.5	0.10	0		

Table 4 (continued)

Mix ratio (lb/gal)		CFR ^a	GS ^b	FSL ^c	Corrected UCS ^d		
Ingredient	Cement				28 d ^e	TC ^f	C ^g
<i>Slaked lime, Type II-LA Portland cement</i>							
3.47	0.53	162	30.	2.8	0		
		153	27.5	2.4	0		
		149	19.5	3.0	0		
<i>Sika liquid admixtures, Type II-LA Portland cement</i>							
15. wt % ^h	2.	9	1.	71.	82	184	80
		10	1.5	61.	64	137	92
		10	1.5	33.	96	109	74
15. wt % ^h	15.	39	3.5	7.3	1268	1333	1298
		34	5.5	5.7	1415	1990	1455
		33	7.	0.96	1306	1455	1440
<i>Masterbuilders liquid admixtures, Type II-LA Portland cement</i>							
15. wt % ^h	2.	9	1.5	68.	95	129	51
		8	1.3	65.	82	76	101
		8	1.3	65.	60	91	68
15. wt % ^h	15.	28	15.5	5.2	1192	1643	1803
		29	17.8	2.2	1033	2463	1653
		27	35.5	0.14	1798	2440	2273

^aCritical flow rate, gal/min.

^b10-min gel strength, lb_f/100 ft².

^c28-d freestanding liquid, vol %.

^dUnconfined compressive strength corrected to a 2-in. cube, psi.

^eAfter curing 28 d.

^fAfter thermal cycling.

^gComparator sample, same age as thermal cycled sample but not subjected to thermal cycling.

^hWeight percent of the admixture in the combination of 106-AN and admixture. The cement mix ratio is pounds of cement per gallon (106-AN + admixture).

additive per gal for seven dry-solids candidates: (1) Class F fly ash, (2) attapulgite clay, (3) Standard Slag GABFS, (4) Takahashi GABFS, (5) ground limestone, (6) sodium silicate, and (7) slaked lime. Not surprisingly, the other two dry-solids candidates—sand and ABFS

aggregate—were too coarse to stay suspended. This prevented meaningful Fann viscometer testing and led to gross segregation in grouts made with these materials. Therefore, these two materials were dropped from the study and were not tested further. The remaining new grouts for Phase II were made up of the liquid admixtures added to the surrogate 106-AN and mixed with the binder at 2 and 15 lb/gal. Each of three admixtures—fluidizer, set retarder, and air entrainer—for each vendor was combined with the 106-AN at 5 wt % each for a total of 15 wt % of liquid admixture in the 106-AN. The vendors recommended less admixture than that used; therefore these results must not be taken as typical for the admixtures. The purpose was to verify the advertised effects qualitatively on grout properties. Individual admixture effects and interaction effects were not tested. In general, the admixture combinations had the expected effect.

The selected vertex grouts for attapulgite clay and slaked lime could not be made and tested, leading to adjustments in the composition for these two additives. The original blends for attapulgite and slaked lime had to be diluted to a total mix ratio of 2 and 4 lb/gal respectively. This brought the binder mix ratio below the constrained minimum of 2 lb of binder per gal for both grouts, leading to the observed weak products (i.e., the slaked lime grout never set and was a soft mush after 28 d). Two new blends were tested for these two: (1) a composition of 13 lb binder per gal and 2 lb of attapulgite per gal, and (2) 11 lb of binder per gal and 4 lb of slaked lime per gal. The new attapulgite grout mixed satisfactorily and properties were measured for it, but it was a thick grout. The new slaked lime grout “flash set” and hardened before any properties could be measured. Based on these results, attapulgite was constrained to a maximum of 2 lb/gal, and the slaked lime was dropped from consideration as being too unstable in these grout mixes.

The sodium silicate grout expanded, cracked, and crumbled during the cure at 90°C, leaving a weak product that crumbled in one’s hand. This was likely caused by an accelerated reaction forming expansive silica gels because of the presence of sodium hydroxide in the 106-AN and soluble silica in the sodium silicate. The freestanding liquid samples that were cured at 40°C did not exhibit the destructive expansive behavior observed at 90°C. The advantage of sodium silicate for control of freestanding liquid was obvious at 40°C: the samples quickly exhibited a smooth firm surface with no hint of moisture. It is not clear what temperature triggers the destructive expansion observed at 90°C. Based on these results, sodium silicate would be a bad choice for 106-AN grouts unless extreme measures were taken to control the grout temperatures. Because temperature control is a known problem for 106-AN grouts, sodium silicate must be ruled out.

Evaluating the results was more complicated for Phase II than for Phase I. Phase I was a straightforward comparison of binders, the objective of which was selecting only one for use in Phases II and III. Phase II involved selecting nonbinder ingredients from among the 14 candidates. Selecting which ingredients to use in Phase III was not straightforward because candidates could not always be directly compared. In other words, different ingredients became candidates for different reasons. For example, attapulgite and sodium silicate were being tested to help control freestanding liquid; therefore it would be fair to compare these two head to head for their effect—not only on freestanding liquid performance but also on other properties such as compressive strength. It would not have been fair to evaluate the effect of attapulgite clay on compressive strength against that of fly ash. Fortunately, this evaluation was simplified by the rejections made during Phase II for reasons already noted.

Reviewing these rejections, sand and ABFS aggregate were rejected because the coarseness of these materials was projected to lead to solid suspension problems during processing, slaked lime was rejected because of potential grout instability, and sodium silicate was rejected because of potential expansion and cracking of the grout. These rejections left fly ash, attapulgite, GABFS, ground limestone, and the admixtures as the nonbinder ingredients still in contention. It was decided a priori to select four dry solids, each with a different purpose: (1) the binder selected in Phase I (i.e., Type II-LA Portland cement), (2) a soluble silica source (i.e., pozzolan) to consume the sodium hydroxide in the 106-AN and calcium hydroxide produced by the hydrating cement, (3) a free-liquid control agent, and (4) an inert filler to dilute the heat evolvers while maintaining the solids content. The admixtures were not to be used unless some help with rheology, set retardation, or thermal cycling performance were needed. (Retarding set over a longer time may have allowed enough heat loss in the vault to prevent grout temperatures from exceeding the preferred limit of 90°C.)

Of the remaining ingredients, only Class F fly ash was a suitable pozzolan, and only attapulgite was a suitable free-liquid control agent. The only choice remaining was to choose either GABFS or ground limestone as the inert filler. First-degree polynomial models were generated using Lotus 1-2-3 from the data in Table 4 for these two ingredients blended with the cement binder and from the data in Table 2 for Type II-LA Portland cement. The models for the critical flow rate, the 10-min gel strength, the 28-d freestanding liquid, and the corrected 28-d unconfined compressive strength are given in Eqs. 15 through 18. The coefficient standard deviations are given in parentheses below each coefficient.

$$\text{CFS} = -1.49 + 3.41 W_1 + 3.59 W_4 + 2.64 W_8 + 2.79 W_9 \quad (15)$$

(0.05) (0.05) (0.05) (0.05)

$$\text{RMSE} = 0.82$$

$$R^2 = 0.998$$

$$\text{GS} = -4.08 + 2.71 W_1 + 1.94 W_4 + 1.49 W_8 + 1.37 W_9 \quad (16)$$

(0.06) (0.06) (0.06) (0.06)

$$\text{RMSE} = 0.92$$

$$R^2 = 0.996$$

$$\text{FSL} = 71.9 - 4.79 W_1 - 4.77 W_4 - 4.64 W_8 - 4.35 W_9 \quad (17)$$

(0.03) (0.03) (0.03) (0.03)

$$\text{RMSE} = 0.54$$

$$R^2 = 0.9997$$

$$\text{UCS} = -387 + 260 W_1 + 18 W_4 + 8 W_8 + 18 W_9 \quad (18)$$

(7) (7) (7) (7)

$$\text{RMSE} = 117$$

$$R^2 = 0.995$$

where

W_4 = mix ratio of the Takahashi GABFS, lb/gal;

W_8 = mix ratio of the Standard Slag GABFS, lb/gal;

W_9 = mix ratio of the ground limestone, lb/gal.

As previously noted, two sources of the air-cooled slag, GABFS, were tested. These models are not necessarily accurate predictors but were intended to provide a means of ranking the effect of different components against each other.

No model was generated for the TC/C ratio because the high ratio for ground limestone was misleading. This high ratio was the result of a dramatic increase in strength for the thermally cycled samples. The strengths of the comparator samples decreased slightly below that at 28 d. The GABFS samples were stronger after thermally cycling than either at 28 d or for the comparator samples—typical behavior for many of the samples tested. Drying the weak cured limestone samples apparently strengthened them, perhaps because of salt precipitation and hardening of hydrates. Increased strength during thermal-cycle testing was typical but usually not as dramatic as with the limestone samples. This response may be

more a reflection of the initial weakness of the limestone grout than a positive response to thermal cycling.

Subsection 5.2 discusses the only adiabatic calorimetry testing done during Phases I and II. Figure 2 illustrates the adiabatic temperature profiles of fly ash blended with ground limestone, Takahashi GABFS blended with ground limestone, and cement blended with ground limestone. The cement was highly exothermic, the fly ash was moderately exothermic, and the GABFS was slightly exothermic. Limestone alone (not illustrated in Fig. 2 or Fig. 3) had a flat profile and, hence, was neither exothermic nor endothermic. Figure 3 illustrates the adiabatic temperature profiles of attapulgite blended with ground limestone. The attapulgite was slightly endothermic.

With this small subset of data, the comparisons between limestone and GABFS can easily be seen using either Table 4 or the coefficients in Eqs. 15 through 18. The ground limestone had a slight advantage in heat evolution: no heat evolved compared with a little for GABFS. The GABFS had a slight advantage with less freestanding liquid. The ground limestone had a slight advantage in rheology (i.e., critical flow rate and 10-min gel strength), but both grouts were well within the preferred limits even at these high-mix ratios. The GABFS did not contribute much to the strength, but the limestone detracted from the strength, putting it at a disadvantage for this property. Either material was a viable inert filler. Selection of ground limestone favors minimizing even modest increases in heat at the expense of modest increases in freestanding liquid and modest decreases in strength (vice versa for selecting GABFS).

Without a clear-cut choice, some subjective observations were worth noting. The current lack of a commercial market for GABFS favors ground limestone. ABFS was readily available, suppliers were willing to specially mill some for testing, and apparently they are willing to mill large quantities for solidifying 106-AN; but it would not be easy to change suppliers.

Ground limestone was generally viewed with disfavor as a potential ingredient within the grout technology community, favoring GABFS. This negative reaction was not readily quantifiable. The consensus appeared to be that it made "bad grout," but why was not clear. The reason may have been that limestone weakens grout, an effect observed in this study. However, this application was unusual in the high initial temperature of the waste and the restrictive upper limit of 90°C. Under such severe constraints, it was understandable that the composition might have to be adjusted such that the freestanding liquid approached its upper

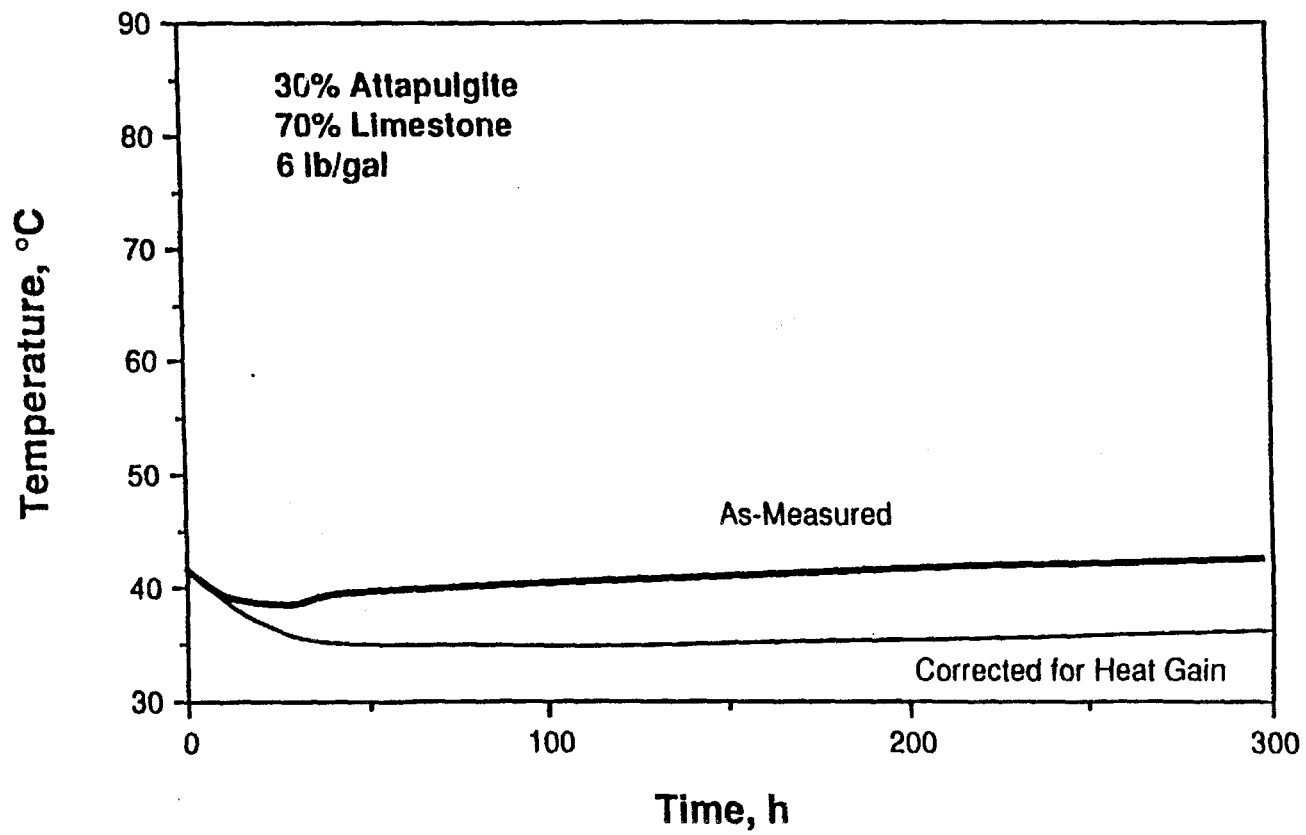


Fig. 3. Adiabatic temperature rise of attapulgite blended 30:70 with ground limestone and mixed at 6 lb/gal with surrogate 106-AN.

limit and the strength approached its lower limit. In other words, this general disfavor might not have been applicable for this special application.

The “bad reputation” of limestone may be a holdover from construction cement and concrete technology. Some limestones contribute to the alkali-aggregate reactions that are to be avoided in construction and waste disposal applications. These are usually impure limestones, and the magnesium content tends to be associated with these expansive reactions. The ground limestone tested was essentially pure calcium carbonate (much better than the 80% specified in the ASTM specifications), and no evidence of alkali reactions with the limestone was noted. In fact, the adiabatic calorimetry indicated the ground limestone was essentially nonreactive with the surrogate 106-AN, a high-alkali solution.

Another unfavorable reaction that is known to occur between limestones and cements is the formation of carboaluminates, but, once again, the calorimetry data indicated that if this reaction were occurring, it had no measurable heat generation. Perhaps carboaluminates contributed to the observed weaker products, higher freestanding liquids, and exaggerated thermal cycling performance of the limestone grout.

Ground limestone is being considered as a substitute for gypsum in Portland cements to control the setting reactions, preventing “flash set” and allowing time to pour the fluid mix into place. The calorimetry data did not indicate any abnormal delays in hydration reactions for the cements mixed with the ground limestone (all of the materials were mixed with limestone for the Phases I and II calorimetry). The GGBFS delay was not unusual because granulated slag must be activated prior to reacting as a cement. This proposed use was controversial because of the aversion by the cement industry to mixing ground limestone with cement; and even then, a strict upper limit (of about 5 wt %) was proposed, ostensibly to prevent carboaluminate formation and any other adverse reactions.

GABFS was selected as the inert filler for further 106-AN grout development. A case could have been made for either material. The ground limestone has already been tested in a 106-AN formulation previously developed; therefore much has already been learned about using limestone with 106-AN. Not surprisingly, this formulation did make a weak product that had trouble with freestanding liquid. The limestone helped control the heat evolution but still had trouble staying below 90°C. By selecting GABFS for this study, a data base will be generated for it, giving two materials at Hanford that have been tested as inert fillers. If necessary, limestone could be tested again and by proper design of the mixture experiment; the effect of dropping the inert filler from the recipe was explored and kept as an option throughout the study. In summary, the dry-solids ingredients selected for the 106-AN grout

formulation development were Type II-LA (moderate heat of hydration) Portland cement, Class F fly ash, attapulgite 150 drilling clay, and GABFS.

7. PHASE III: MIXTURE EXPERIMENT

7.1 EXPERIMENTAL TEST-PLAN DESIGN

Four ingredients—Type II-LA (moderate heat of hydration) Portland cement, Class F fly ash, attapulgite clay, and GABFS—were selected for development into the 106-AN grout formulation. A preliminary formulation of 2.5, 1.2, 0.8, and 3.5 lb/gal, respectively, of cement, fly ash, attapulgite, and GABFS was recommended. This preliminary formulation was used as the basis for the Phase III mixture experiment design.

7.1.1 Experimental-Design Approaches Considered

Three general approaches were considered for the design of the 106-AN grout-formulation experiment (these approaches correspond to ones that have been widely used in the statistical mixture-experiment literature):

1. *pounds per gallon (ratio) variables*—design experiment in terms of the pounds of dry-blend ingredients per gallon of liquid waste,
2. *mixture amount*—design the experiment in terms of the mass fractions of the dry blend considered as a mixture (with mass fractions summing to 1.0) and the total amount of the dry blend added per gal of liquid waste (the total amount is equivalent to the mix ratio of dry-blend ingredients to liquid waste), and
3. *classical mixture*—design the experiment in terms of the mass fractions of the five grout components (i.e., cement, flyash, clay, slag, and liquid waste).

Not only will these three approaches lead to different experimental designs, but each has a corresponding empirical-model form that is mathematically different than the model forms for the other approaches (the model forms are presented in Subsect. 7.1). However, there was no reason a priori to believe that one model form would fit the resulting grout property data better than the other two model forms; therefore this aspect was not considered further in choosing among the three approaches. Although each of these three approaches

has merit, the first was selected because it was compatible with the definition of the grout composition region to be explored and was based on the commonly used pound-per-gallon basis.

7.1.2 Phase III Experimental Region

Initially, two regions were defined in terms of the mix ratio of each dry-solids ingredient. The larger region was defined by the extreme bounds on the grout composition. Experience indicates that a minimum binder (i.e., cement plus fly ash) content of 2 lb/gal is required ($W_1 + W_2 \geq 2$). Because fly ash does not solidify well alone, a minimum cement content of 1 lb/gal was specified ($W_1 \geq 1$). The Fann viscometer is dependable at solids contents of 15 lb/gal or less, setting the upper bounds on all of the dry solids except attapulgite ($W_1 + W_2 + W_3 + W_4 \leq 15$). Experience indicated that the current criteria limited the attapulgite to 2 lb/gal or less ($W_4 \leq 2$). The smaller region defined a region of compositions expected to come closer to the criteria within the larger region. A summary of these constraints follows:

Constraints			
Larger region		Smaller region	
$1 \leq W_1$	≤ 15	$1.5 \leq W_1$	≤ 3.5
$0 \leq W_2$	≤ 15	$0 \leq W_2$	≤ 6
$0 \leq W_3$	≤ 2	$0.5 \leq W_3$	≤ 2
$0 \leq W_4$	≤ 13	$0 \leq W_4$	≤ 6
$2 \leq W_1 + W_2$		$4 \leq W_2 + W_4$	≤ 6
$W_1 + W_2 + W_3 + W_4$	≤ 15	$W_1 + W_2 + W_3 + W_4$	≤ 10

where

- W_1 = mix ratio for cement, lb/gal;
- W_2 = mix ratio for fly ash, lb/gal;
- W_3 = mix ratio for attapulgite, lb/gal;
- W_4 = mix ratio for GABFS, lb/gal.

The "larger region" was defined to push the limits of feasible grout formulations and thereby gain the greatest knowledge of how the dry-blend components affect grout

properties. The “smaller region” (inside the “larger region”) was defined to represent prior knowledge about the range of desirable grout formulations more closely and was designed around the preliminary recommended formulation. As discussed in the next subsection, eventually the smaller region was the sole basis for the grout-formulation experimental design selected.

Note that both regions are defined in terms of “lower and upper bounds” on W_1 through W_4 (the pound-per-gallon dry-blend components) individually as well as on sums of these components. Geometrically, each region is an irregular polyhedron. Lower and upper bounds on individual components define a four-dimensional box, and then the lower and upper bounds on the sums of the components cut off corners of the box leaving an irregular polyhedron.

7.1.3 106-AN Experimental Design

Two experimental designs were generated via statistical methods—the primary design (containing formulations from both the larger and smaller regions) and a second “back-up” design (containing only formulations from the smaller region). The first experimental design was initially chosen, but then based on preliminary results and additional considerations, the backup design was adopted. The statistical methods used to generate this design (see Table 5) and the design itself are discussed below.

Statistical “optimal experimental design” methodology and software were used to generate the design listed in Table 5 as outlined in the following steps:

1. The extreme vertices and various dimensional centroids of the smaller region* were generated using the MIXSOFT package⁴ routines MCCVRT and AEVC. The vertices and centroids were then combined to form a set of candidate grout formulations.
2. An 18-grout design was selected from the candidate set using “optimal statistical design” software. Both the MIXSOFT and ACED⁵ packages were used to select and

*Extreme vertices and 1-, 2-, and 3-dimensional centroids are merely grout formulations on the boundary of the experimental region.

Table 5. 106-AN grout development experimental design for the smaller region only

No.	Random run No.	ORNL No.	W ₁	W ₂	W ₃	W ₄	Description of formulation ^a	
			(lb/gal of liquid waste)					
			Cement	Fly ash	Attapulgate clay	Slag		
1	3	10	1.5	0.0	2.0	6.0	SR vertex	
2	8	23	1.5	6.0	2.0	0.0	SR vertex	
3	12	27	3.5	0.0	0.5	6.0	SR vertex	
4	6	21	3.5	6.0	0.5	0.0	SR vertex	
5	19	34	1.5	0.0	0.5	4.0	SR vertex	
6	15	30	1.5	4.0	0.5	0.0	SR vertex	
7	20	35	3.5	0.0	2.0	4.0	SR vertex	
8	17	32	3.5	4.5	2.0	0.0	SR vertex	
9	1	1	1.5	0.0	1.25	6.0	SR edge centroid	
10	11	26	1.5	3.0	0.5	3.0	SR edge centroid	
11	14	29	1.5	2.0	2.0	2.0	SR edge centroid	
12	10	25	3.5	2.0	0.5	2.0	SR edge centroid	
13	13	28	2.5	6.0	0.5	0.0	SR edge centroid	
14	18	33	2.5	4.0	2.0	0.0	SR edge centroid	
15	16	31	1.5	5.0	1.25	0.0	SR 2-dim. centroid	
16	7	22	2.5	0.0	0.5	5.0	SR 2-dim. centroid	
17	4	15	2.75	2.625	2.0	2.625	SR 2-dim. centroid	
18	9	24	2.75	3.0	1.25	3.0	SR 2-dim. centroid	
19	2	7	2.5	1.2	0.8	3.5	SR "reference" formulation	
20	5	20	2.444	2.472	1.333	2.472	SR overall centroid	

^aSR = smaller region.

to evaluate many 18-grout designs that had "close to optimal" statistical design criteria values.* One design was selected.

*The main statistical criterion used was that of "minimizing the maximum prediction variance" over the experimental region. Clearly, it is desirable to minimize the uncertainty of predictions to be made with the fitted empirical grout property models.

3. Two additional grouts representing a recommended formulation and the “center” of the design region were added to the design.

Note that the 18 grout formulations selected using the statistical “optimal experimental design” approach (i.e., the first 18 grouts in Table 5) are all on the boundary of the smaller experimental region. There are eight extreme vertices (i.e., corner points of the polyhedral region), six edge centroids, and four two-dimensional face centroids. Only grouts on the boundary of the experimental region were generated and selected because they best minimize the uncertainties of predictions to be made with the models fitted to experimental data. It would also have been desirable to include additional points on the interior of the experimental region to increase the potential for obtaining accurate models.

As it stands, this design is “minimal” in that there are only five more distinct formulations than terms (i.e., 20 distinct formulations and 15 term second-order models) in any of the second-order models that might be used to fit the data. Typically, it is preferable to have at least 10 to 15 more distinct design points than model terms to provide for better assessment of model adequacy. In this case the assessment of model adequacy is being evaluated through additional testing.

7.1.4 Replication and Randomization

The procedure for making the formulations included making three replicates. The replicates for each formulation came from one blend of the dry materials. Each replicate consisted of a portion of the dry blend mixed with the waste individually but consecutively. Randomization of the order of measurement of the grout properties is desirable. For example, unconfined compressive strength would not be measured consecutively on three replicates of the same formulation. Ideally, this randomization would be completely independent of the randomization employed during formulation. However, because all of the grout properties are measured at a fixed time after formulation (e.g., 10-min gel strength), the measurements for this design depended on the order of formulation. Consequently, the three replicates of each formulation were measured one after the other, and the longer-term *measurement* sources of variation that may be present are not accounted for in the estimate of the experimental uncertainty, the consequences of which are discussed in Subsect. 7.2.

7.2. RESULTS

Table 6 lists the critical flow rate, the 10-min gel strength, the 28-d freestanding liquid, the 28-d unconfined compressive strength, and the nitrate plus nitrite leachability index results of the mixture experiment for the grouts in Table 5. Table 7 lists the temperature rise of these grouts after 10, 24, 100, 200, and 300 h of hydration. Because the calorimeters can measure temperatures only up to 98°C, some of the values listed in the table are extrapolations.

7.3 STATISTICAL METHODS FOR DEVELOPING GROUT PROPERTY MODELS

This subsection discusses the statistical methods used in modeling and analyzing the data from the 106-AN experimentation. The grout properties addressed are critical flow rate, 10-min gel strength, 28-d freestanding liquid, unconfined compressive strength, leachability index for $\text{NO}_3 + \text{NO}_2$, and adiabatic calorimetry. The basic steps of analysis are listed below (each one is explained in detail in the subsections following):

1. Three second-order model forms were considered.
2. Least squares regression was used to fit models to data.
3. Outliers and possible transformations of the grout properties were identified. This step is an iterative process used to convince the analyst that the assumptions of least squares regression have been met and that the best possible fit has been obtained.
4. The final full and reduced models were fit to the data and evaluated for the quality of the fit.
5. Uncertainty in the model predictions was quantified.

7.3.1 Empirical-Model Forms Considered

Each of the three design approaches discussed in Subect. 7.1.1 has corresponding second-order empirical models that are not mathematically equivalent. Although the first design approach was chosen, empirical model forms corresponding to all three approaches were investigated. Because the three model forms are not equivalent, the potential exists that one might fit the data better than the others.

Table 6. Phase III: Results for the 106-AN mixture-experiment grouts

ORNL No.	Critical flow rate (gal/min)	10-min gel strength (lb _f /100 ft ²)	28-d free-standing liquid (vol %)	28-d corrected unconfined compressive strength (psi)	Nitrate + nitrite leachability index
1	33.	14.5	2.26	270.	5.5
	34.	14.5	2.61	265.	5.4
	33.	14.5	2.01	258.	5.5
7	20.	9.5	8.23	243.	5.6
	20.	8.5	3.99	285.	5.4
	20.	9.5	7.15	326.	5.6
10	109.	27.5	0.38	328.	5.7
	104.	27.5	0.51	315.	5.6
	107.	28.5	0.22	328.	5.6
15	70.	22.5	0.19	877.	5.7
	70.	23.5	0.22	823.	5.7
	71.	23.5	0.13	846.	5.7
20	33.	13.5	0.56	468.	5.8
	33.	15.5	1.19	391.	5.8
	33.	14.	0.32	457.	5.9
21	23.	12.	0.26	2125.	6.3
	23.	14.5	1.73	1913.	6.6
	24.	12.5	1.38	1780.	6.5
22	17.	11.5	7.72	340.	5.7
	18.	12.	9.67	358.	5.7
	17.	11.5	11.63	305.	5.7
23	454. ^a	22. ^a	0.13	1065.	6.7
	128.	14.5	0.13	1080.	6.7
	130.	16.5	0.10	1064.	6.8
24	29.	14.	1.40	497.	5.6
	39.	17.5	0.53	670.	5.7
	38.	17.	0.53	680.	5.8
25	18.	8.5	3.05	631.	5.7
	18.	9.	5.18	570.	5.7
	18.	9.5	7.22	588.	5.7
26	17.	8.5	6.30	484.	6.2
	16.	9.	9.23	391.	5.9
	17.	8.5	6.70	398.	5.9

Table 6 (continued)

ORNL No.	Critical flow rate (gal/min)	10-min gel strength (lb _f /100 ft ²)	28-d free-standing liquid (vol %)	28-d corrected unconfined compressive strength (psi)	Nitrate + nitrite leachability index
27	24.	17.	4.31	584.	5.7
	24.	16.5	3.43	541.	5.7
	25.	16.	4.21	546.	5.7
28	18.	8.	5.08	1326.	6.0
	18.	6.	6.03	1407.	6.1
	18.	9.	8.01	1226.	5.8
29	62.	20.	0.10	422.	6.1
	63.	19.5	0.16	431.	6.0
	62.	19.5	0.22	411.	6.0
30	11.	1.5	17.65	733.	5.6
	11.	1.8	18.05	657.	5.6
	11.	1.8	19.97	603.	5.6
31	27.	8.	0.29	629.	5.7
	27.	8.5	0.32	637.	5.7
	27.	8.	0.42	636.	5.9
32	76.	22.5	0.13	1705.	6.6
	75.	21.	0.17	1680.	6.5
	75.	22.5	0.06	1548.	6.6
33	66.	17.5	0.13	964.	5.9
	66.	19.5	0.13	912.	5.9
	65.	21.5	0.13	1017.	6.2
34	11.	5.5	20.91	151.	5.5
	12.	4.5	19.84	158.	5.5
	11.	4.5	18.96	138.	5.5
35	67.	30.	0.13	685.	5.8
	69.	28.5	0.13	926.	5.9
	68.	27.5	0.13	820.	6.0

^aThe Fann viscometer rotor/bob combination was changed for Batches 2 and 3 because the grout was almost too thick for the combination used for Batch 1.

**Table 7. Measured adiabatic temperature rise of
106-AN grouts, °C**

Grout No.	10 h	24 h	100 h	200 h	300 h
1	13.1	15.5	20.4	25.6	28.2
10	13.7	15.7	21.6	25	26.4 ^a
21	34.8	45.3	57	60.6	62
22	20	23.7	31.1	35.9	38.1 ^a
23	24.6	40.7	46	48.8 ^a	50.2 ^a
24	27.6	38.1	52.2	59.8	62.7
25	28.6	35.4	53.2	71.1	85
26	14.3	24.3	37.3	43.7	47.4 ^a
27	25.6	30.5	41.1	49.2 ^a	55.3 ^a
28	25.8	41.3	61.5	67.9	69.2
15	29.5	40.7	53.1	63.2	66.5
29	18.3	25.9	36.9	38.3	38.5
30	9.5	26.3	42	50.1	52.7 ^a
31	20	34.3	42.9	46.7	47.7 ^a
32	36.5	48.1	61.2	68.2	70.9
33	30.8	44.1	51.2	57.1	61
34	10.1	13.3	18.8	21.8	23.8
35	24.1	28.4	39.9	44.6	48.8
7	22.6	28	40.3	46.1	51
15	27.3	39.1	50.1	55.6 ^a	58. ^a
20	25.3	35.6	47.2	52.8 ^b	55.2

^aValues extrapolated with a good deal of confidence.

^bValues extrapolated with little confidence because of the shape of the curves and the short time periods of the actual runs.

The second-order empirical models that correspond to the three design approaches follow (the surrogate 106-AN solution has a density of 10 lb/gal):

1. *Second-Order Polynomial Model* (expressing dry-blend ingredients as pounds per gallon of waste)

$$\eta = \beta_0 + \beta_1 W_1 + \beta_2 W_2 + \beta_3 W_3 + \beta_4 W_4 + \beta_{12} W_1 W_2 + \beta_{13} W_1 W_3 + \beta_{14} W_1 W_4 \\ + \beta_{23} W_2 W_3 + \beta_{24} W_2 W_4 + \beta_{34} W_3 W_4 + \beta_{11} W_1^2 + \beta_{22} W_2^2 + \beta_{33} W_3^2 + \beta_{44} W_4^2$$

where W_1 through W_4 are as defined in Subsect. 7.1.2.

2. *Mixture-Amount Model* (treating dry-blend ingredients as a mixture)

$$\eta = \beta_1 V_1 + \beta_2 V_2 + \beta_3 V_3 + \beta_4 V_4 + \beta_{12} V_1 V_2 + \beta_{13} V_1 V_3 + \beta_{14} V_1 V_4 + \beta_{23} V_2 V_3 \\ + \beta_{24} V_2 V_4 + \beta_{34} V_3 V_4 + \beta_1^1 V_1 MR + \beta_2^1 V_2 MR + \beta_3^1 V_3 MR + \beta_4^1 V_4 MR \\ + \beta_0^2 MR^2$$

where

$$V_1 = W_1 / (W_1 + W_2 + W_3 + W_4), \\ V_2 = W_2 / (W_1 + W_2 + W_3 + W_4), \\ V_3 = W_3 / (W_1 + W_2 + W_3 + W_4), \\ V_4 = W_4 / (W_1 + W_2 + W_3 + W_4), \\ MR = \text{mix ratio} = W_1 + W_2 + W_3 + W_4, \\ V_1 + V_2 + V_3 + V_4 = 1.$$

3. *Second-Order Scheffé Model* (treating all ingredients as a mixture)

$$\eta = \beta_1 X_1 + \beta_2 X_2 + \beta_3 X_3 + \beta_4 X_4 + \beta_5 X_5 + \beta_{12} X_1 X_2 + \beta_{13} X_1 X_3 + \beta_{14} X_1 X_4 \\ + \beta_{15} X_1 X_5 + \beta_{23} X_2 X_3 + \beta_{24} X_2 X_4 + \beta_{25} X_2 X_5 + \beta_{34} X_3 X_4 + \beta_{35} X_3 X_5 \\ + \beta_{45} X_4 X_5$$

where

$$X_1 = W_1 / (W_1 + W_2 + W_3 + W_4 + 10), \\ X_2 = W_2 / (W_1 + W_2 + W_3 + W_4 + 10), \\ X_3 = W_3 / (W_1 + W_2 + W_3 + W_4 + 10),$$

$$X_4 = W_4 / (W_1 + W_2 + W_3 + W_4 + 10),$$

$$\begin{aligned} X_5 &= \text{percentage of waste lb/gal to the total lb/gal} \\ &= 10 / (W_1 + W_2 + W_3 + W_4 + 10), \end{aligned}$$

$$X_1 + X_2 + X_3 + X_4 + X_5 = 1.$$

In all models η denotes an untransformed or transformed grout property.

These empirical models were initially fitted to one of the grout properties (critical flow rate) and evaluated using standard statistical methods. A conclusive decision regarding the best model option could not be made using the data available. The ideal way to determine which model is best would be to have a data set, not used in the estimation of the model coefficients, that could be used to validate the prediction capabilities of each model. Such a validation data set was not available. Alternately, with large numbers of observations, a validation data set can be simulated (referred to as cross-validation) when not available. However, the 20 design points in the grout formulation study are too few to employ cross-validation. Therefore, the second-order polynomial model was chosen as “best” because it corresponds to the approach used in designing the experiment. Thus, for all grout properties, the second-order polynomial model was used.

7.3.2 Least-Squares Regression

Unweighted least-squares regression was used to fit all models to the data. The method of least squares takes the “best fitting” model to be the one that comes closest to the data in the sense of minimizing the sum of squared differences between the observed values and the values predicted by the model. The assumptions of least-squares regression are that the model is structurally adequate and that the errors are independent, normally distributed, and have constant variance.⁶

7.3.3 Identification of Outliers and Transformations

Residuals (i.e., differences between measured and model-predicted property values) were plotted versus the predicted values. Residual plots are used to check that the errors are normally distributed with mean zero and constant variance. Any patterns identified in the residual plot indicate a possible problem with the appropriateness of the model or the least-squares assumptions. Residual plots are also used to identify outliers.

A property (i.e., dependent variable) transformation might be used to satisfy the assumption of constant variance or to improve the overall fit of the model. The Box-Cox procedure⁷ was applied to help determine whether transformations of the grout properties may be appropriate and to indicate what transformations would be best. The procedure is also able to indicate if one transformation is better than another (e.g., it can indicate whether taking the log transformation would result in a significant gain in fit over the square root transformation). Information from residual plots and from plots of predicted versus measured values can also be used to determine transformations.

The Box-Cox procedure calculates the sum of the squared residuals (RSS) using several transformations such as the natural log or the square root. The RSS for each transformation is compared with the others, and the transformation that corresponds to the smallest RSS is chosen as best. There are methods of incorporating uncertainty in these estimates of RSS and calculating a 95% confidence interval to cover a range of transformations that are “good.”

7.3.4 Quality of Fit for Full and Reduced Models

A consequence of fitting a 15-term second-order polynomial model to 20 distinct formulations is that the design may be overfit. If the number of distinct formulations was *equal* to the number of model coefficients, the model would fit the data exactly (except for replicate variability, called experimental uncertainty). For this study, having five more formulations than terms in the full second-order model will help, but the risk of overfitting is present and can lead to inaccurate predictions at points not used to fit the model.

Overfitting can be identified using several techniques. A quick check is to look at the tests of significance for the coefficient estimates. If more than a few of the coefficient estimates are nonsignificant, the model may be overfit. Techniques designed to drop explanatory variables that have little or no effect on the grout properties from the model have been employed to reduce the potential for overfitting.

Once a “final” reduced model is determined, a last check of the quality of the fit is appropriate. This is done through what is called a lack-of-fit test. This test is possible when formulations have been replicated during experimentation. These replicates are used to estimate the experimental uncertainty in the data (referred to as “pure error”). Pure error sum of squares represents the contribution to the residual error sum of squares that is due to such things as sample preparation variability, mixing and blender variability, technician

variability, and measurement uncertainty. When the pure error sum of squares is partitioned out of the residual error sum of squares in regression, what is left is called the lack-of-fit sum of squares. The hypothesis that the lack-of-fit error is approximately equal to the pure error is then tested statistically. If the hypothesis is rejected, then the model is said to have a significant lack of fit.

The validity of the lack-of-fit test depends heavily on the estimate of pure error and thus on the quality of the replications during the experiment. Since the formulations for the 106-AN experiment were not replicated over all possible sources of variation, the estimate of pure error may be significantly biased below the true value. Consequently, a statistically significant lack of fit may be a “false alarm,” and it will be necessary to subjectively ascertain whether the lack of fit is practically significant or not.

7.3.5 Uncertainty in the Model Predictions

The fitted models can be used to predict values of unconfined compressive strength, 10-min gel strength, critical flow rate, 28-d freestanding liquid, leachability, or adiabatic calorimetry anywhere within the compositional region. However, these predictions will be subject to the experimental uncertainty involved in the least-squares modeling process. Least-squares theory provides for quantifying the standard deviation of any prediction; thus, statistical statements such as 95% confidence intervals or 95% prediction intervals can be made. A 95% confidence interval is obtained by treating the prediction as a mean; a 95% prediction interval, by treating the prediction as an individual observation. The formulas for computing these two types of statistical intervals for predictions are given in Appendix C.

Both 95% confidence and prediction intervals are statements about property values for one formulation at a time. Statements about many or all possible formulations at a time are also possible (referred to as confidence bands and prediction bands) but are not discussed here. Similarly, 95/95 tolerance intervals (or bands) that make a 95% confidence statement about 95% of the potential distribution of property values for a given formulation can also be constructed but are not discussed here.

7.4 RESULTS OF MODELS FITTED TO GROUT PROPERTIES

The subsections that follow contain specific information on the statistical analysis and modeling of each grout property. This includes results from each step of the data analysis. The definitions for the component variables are repeated here:

W_1 = mix ratio for cement, lb/gal;

W_2 = mix ratio for fly ash, lb/gal;

W_3 = mix ratio for attapulgite, lb/gal;

W_4 = mix ratio for GABFS, lb/gal.

Modeling was attempted on the untransformed and the transformed dependent properties, but modeling was always first attempted on the former. No clear winner was evident in the statistical comparison between the untransformed and the transformed models for the critical flow rate and unconfined compressive strength; therefore both models are discussed.

7.4.1 Critical Flow Rate

Critical flow rate data (see Table 6) were fitted to the full second-order model with the 1/square root (SQRT) transformation (as suggested by the Box-Cox procedure) and with no transformation. Observation No. 22 was omitted from the analysis because of its extreme value (454 gal/min). The point was measured under unique circumstances. This grout was so thick that higher Fann viscometer rpms could not be measured, and the rotor/bob combination was changed for the two duplicate batches. With the 1/SQRT transformation, another point (i.e., observation No. 25, 29 gal/min) was identified as a possible outlier. The transformed property was analyzed with and without that point; because no significant difference in results was apparent, the point was left in. The lack of fit was statistically significant for both models, but the test may give false alarms because of the potential bias in the estimate of pure error. The lack of fit may not be practically significant given knowledge about the uncertainties.

Model-reduction techniques were applied to the full models. The model with the transformed critical flow rate was used as the dependent variable. The untransformed model

and the final model for 1/SQRT (critical flow rate) follow (see Appendix B, Table B.1, for details):

Critical Flow Rate (CFR), gal/min

Transformed Model

$$\frac{1}{\sqrt{\text{CFR}}} = 0.589 - 0.072 W_1 - 0.040 W_2 - 0.178 W_3 - 0.042 W_4 + 0.007 W_1 W_2 \\ + 0.021 W_1 W_3 + 0.007 W_1 W_4 + 0.007 W_2 W_3 + 0.009 W_3 W_4$$

Critical Flow Rate (CFR), gal/min

Untransformed Models

$$\text{CFR} = 3.71 + 25.1 W_1 - 0.970 W_2 - 98.5 W_3 + 2.70 W_4 - 4.09 W_1 W_2 - 5.43 W_1 W_3 \\ - 3.24 W_1 W_4 + 12.5 W_2 W_3 + 11.1 W_3 W_4 + 0.904 W_2^2 + 38.7 W_3^2$$

7.4.2 10-Min Gel Strength

Ten-min gel strength data (see Table 6) were fitted to the full second-order model with the SQRT transformation (as suggested by the Box-Cox procedure) and with no transformation.

Observation No. 22 was omitted from the analysis because of its extreme value (22 lb_f/100 ft²). With the SQRT transformation, another point (observation No. 38, 6 lb_f/100 ft²) was identified as a possible outlier. The point was determined not to be influential to the results and was left in. The lack of fit was significant for both models, but the test may give false alarms because of the potential bias in the estimate of pure error. The lack of fit may not be practically significant given knowledge about the uncertainties.

Model-reduction techniques were applied to the full models. The results indicated that the reduced model for 10-min gel strength without the transformation was more appropriate. The final model for 10-min gel strength is given below (see Appendix B, Table B.2 for details).

10-Min Gel Strength (GELS), lb/100 ft²

$$\begin{aligned} \text{GELS} = & - 9.79 + 3.09 W_1 + 2.09 W_2 - 1.50 W_3 + 2.41 W_4 - 0.72 W_2 W_3 \\ & + 5.25 W_3^2 \end{aligned}$$

7.4.3 28-d Freestanding Liquid

Twenty-eight day freestanding liquid data (see Table 6) were fitted to the full second-order model with the natural log (LOG) transformation (as suggested by the Box-Cox procedure) and with no transformation. All observations were used for the analysis with no transformation. With the LOG transformation, observation No. 16 (0.26 vol %) was omitted from the analysis because it was highly influential to the results. With no transformation, the lack of fit was not significant. With the LOG transformation, the lack of fit was significant, but the test may give false alarms because of the potential bias in the estimate of pure error. The lack of fit may not be practically significant given knowledge about the uncertainties.

Model-reduction techniques were applied to the full models. The model with the transformed 28-d freestanding liquid was used as the dependent variable. The final model for LOG (28-d freestanding liquid) is given below (see Appendix B, Table B.3, for details).

28-d Freestanding Liquid (FSL28), Vol %

$$\begin{aligned} \log(\text{FSL28}) = & 6.68 + 1.32 W_1 - 0.61 W_2 - 7.39 W_3 - 0.65 W_4 + 0.37 W_1 W_3 \\ & + 0.34 W_2 W_3 + 0.39 W_3 W_4 - 0.43 W_1^2 + 0.84 W_3^2 + 0.026 W_4^2 \end{aligned}$$

7.4.4 Unconfined Compressive Strength

Unconfined compressive strength data (see Table 6) were fitted to the full second-order model with the SQRT transformation (as suggested by the Box-Cox procedure) and with no transformation. Observation No. 16 was omitted from the analysis because of its extreme value (2125 psi). The lack of fit was significant for both models, but the test may give false alarms because of the potential bias in the estimate of pure error. The lack of fit may not be practically significant given knowledge about the uncertainties.

Model-reduction techniques were applied to the full models. It was decided to use the model with the transformed unconfined compressive strength as the dependent variable. The final model for SQRT unconfined compressive strength is given below (see Appendix B, Table B.4 for details).

Unconfined Compressive Strength (UCS)

Transformed Model

$$\begin{aligned}\sqrt{\text{UCS}} = & 10.92 - 1.29 W_1 + 4.72 W_2 - 13.48 W_3 + 1.50 W_4 + 1.64 W_1 W_3 \\ & - 0.45 W_2 W_3 - 0.42 W_2 W_4 + 0.88 W_1^2 + 5.33 W_3^2\end{aligned}$$

Unconfined Compressive Strength (UCS)

Untransformed Model

$$\begin{aligned}\text{UCS} = & 428 - 333 W_1 + 137 W_2 - 873 W_3 + 91.5 W_4 + 43.0 W_1 W_2 \\ & + 111 W_1 W_3 - 28.0 W_2 W_4 + 75.8 W_1^2 + 292 W_3^2\end{aligned}$$

7.4.5 Leachability for $\text{NO}_3 + \text{NO}_2$

Leach test results can be sensitive to curing procedures. Note that the grouts for this study were cured at 90°C to make the results conservative, and the resulting leachability index measurements covered a very small range. The small range in the grout property response will reduce the effectiveness of the modeling efforts. Several results from the modeling effort indicate that the leachability model is not as good as the models for the other grout properties: (1) The amount of total variability explained by the model (the R^2 value) is only 0.86 for the full 15-term model, while the minimum R^2 for the full 15-term model for the other properties is 0.96. (2) The Box-Cox procedure was not able to identify specifically an appropriate transformation as it had for the other properties.

Leachability for $\text{NO}_3 + \text{NO}_2$ data (see Table 6) were fitted to the full second-order model with no transformation. None of the observations were omitted from the analysis. The lack of fit was significant for this model, but the test may give false alarms because of the

potential bias in the estimate of pure error. The lack of fit may or may not be practically significant.

Model reduction techniques were applied to the full model. The final model for leachability for $\text{NO}_3 + \text{NO}_2$ is given below (see Appendix B, Table B.5 for details).

$$\begin{aligned} \text{NOX} = & 5.41 - 0.92 W_1 + 0.29 W_2 - 0.40 W_3 + 0.59 W_4 - 0.026 W_1 W_4 \\ & - 0.048 W_2 W_4 - 0.079 W_3 W_4 + 0.212 W_1^2 + 0.312 W_3^2 - 0.047 W_4^2 \end{aligned}$$

7.4.6 Adiabatic Calorimetry

The data from the adiabatic calorimetry measurements are considered to be repeated measurements because the same grout was measured at several different time periods—at 10, 24, 100, 200 and 300 h after curing.

The adiabatic calorimetry data were analyzed with the time periods treated as independent responses. Time periods (200 and 300 h) were not analyzed because the majority of the data were extrapolated. Lack-of-fit tests could not be computed because there were no replications for these data. The results for periods 10, 24, and 100 h are listed below.

7.4.6.1 Rise in heat at 10 h

Heat-rise data at 10 h (see Table 7) were fitted to the full second-order model with no transformation. None of the observations were omitted from the analysis. Model-reduction techniques were applied to the full model. The final model for h 10 is given below (see Appendix B, Table B.6 for details).

$$\begin{aligned} \text{HR10} = & - 27.52 + 20.60 W_1 + 1.88 W_2 + 10.68 W_3 + 3.68 W_4 - 2.11 W_1 W_3 \\ & - 0.59 W_1 W_4 - 1.10 W_3 W_4 - 1.87 W_1^2 - 0.11 W_4^2 \end{aligned}$$

7.4.6.2 Rise in heat at 24 h

Heat-rise data at 24 h (see Table 7) were fitted to the full second-order model with no transformation. None of the observations were omitted from the analysis. Model-reduction techniques were applied to the full model. The final model for 24 h is given below (see Appendix B, Table B.7 for details).

$$\begin{aligned} \text{HR24} = & - 20.51 + 21.97 W_1 + 5.05 W_2 + 7.79 W_3 + 1.41 W_4 - 0.955 W_1 W_3 \\ & - 0.96 W_3 W_4 - 2.82 W_1^2 - 0.23 W_2^2 \end{aligned}$$

7.4.6.3 Rise in heat at 100 h

Three of the data points used in this analysis were extrapolated but included in the analysis. Heat rise data at 100 h (see Table 7) were fitted to the full second-order model, but the results were questionable. The reduced model for this property did not require a transformation and looked much more appropriate according to all the statistical tools available for these data. The final model for h 100 is given below (see Appendix B, Table B.8 for details).

$$\text{HR100} = - 8.17 + 24.00 W_1 + 7.78 W_2 - 3.02 W_1^2 - 0.64 W_2^2$$

8. RECOMMENDED 106-AN GROUT FORMULATIONS

Several grouts are recommended in this section based on the predicted properties from the model and the desired properties for operation.

8.1 PREDICTED PROPERTIES IN THE CONSTRAINED REGION

The selection of a grout formulation may be approached in several ways once the final models have been obtained. One graphical technique for displaying and examining the sensitivity of the grout properties to changes in the dry-blend composition as they vary in

the experimental region is to create response-surface contour plots. For each of the grout properties, a region can be identified where the predicted grout property meets a given criteria (uncertainty in the model prediction needs to be accounted for in this process). When these regions are identified for each grout property, they can be overlaid to find the region that satisfies all grout criteria simultaneously, if one exists. Examples of these plots based on the property models (without accounting for uncertainties) are illustrated in Figs. 4 through 6. The blacked-out regions of the plots indicated areas outside of the smaller constrained region.

Over 2000 grout compositions were randomly generated over the smaller constrained region. These compositions were substituted into the model equations, and the predicted properties for these grouts were calculated (see Appendix E). Some general trends were noted by plotting a predicted property for all of these grouts against an individual ingredient. Figs. 7 through 12 illustrate these plots for the “over 2000 random grouts” listed in Appendix E. Wide scatter was expected for these plots since the other ingredients varied as well as the ingredient being plotted. The predicted, significant effect of attapulgit content on the freestanding liquid and critical flow rate are apparent. One must be careful of drawing any conclusions from such plots since (1) these are all calculated properties and (2) the compositions were not completely independent of each other. The fly ash and slag compositions were dependent on each other to a certain degree in that their total mix ratio had to be between 4 and 6 lb/gal. In addition, the overall total mix ratio was restricted to 10 lb/gal. Thus, for higher solids content, adding more of any ingredient had to be done while lowering some other ingredient to stay within the constrained region. This dependency was not as restrictive as the one for fly ash or slag.

Thus, the apparent significant decline in compressive strength predicted with increased slag may be more of an effect of replacing fly ash with the slag. Not unexpectedly, fly ash is predicted to be a significant contributor to the compressive strength. The two heat contributors were cement and fly ash; therefore the predicted calorimetry behavior in Figs. 11 and 12 was not unexpected, and the predicted decline with slag likely results from replacing fly ash.

These plots were useful in recommending grout formulations for 106-AN. Any number of random grouts to generate such plots (or tables) of predicted values can be generated using these equations. The predictive accuracy of these models is being tested with a set of validation grouts. These validation grouts are being tested in the laboratory using the same procedures as those for the mixture experiment. The validation testing may prove that

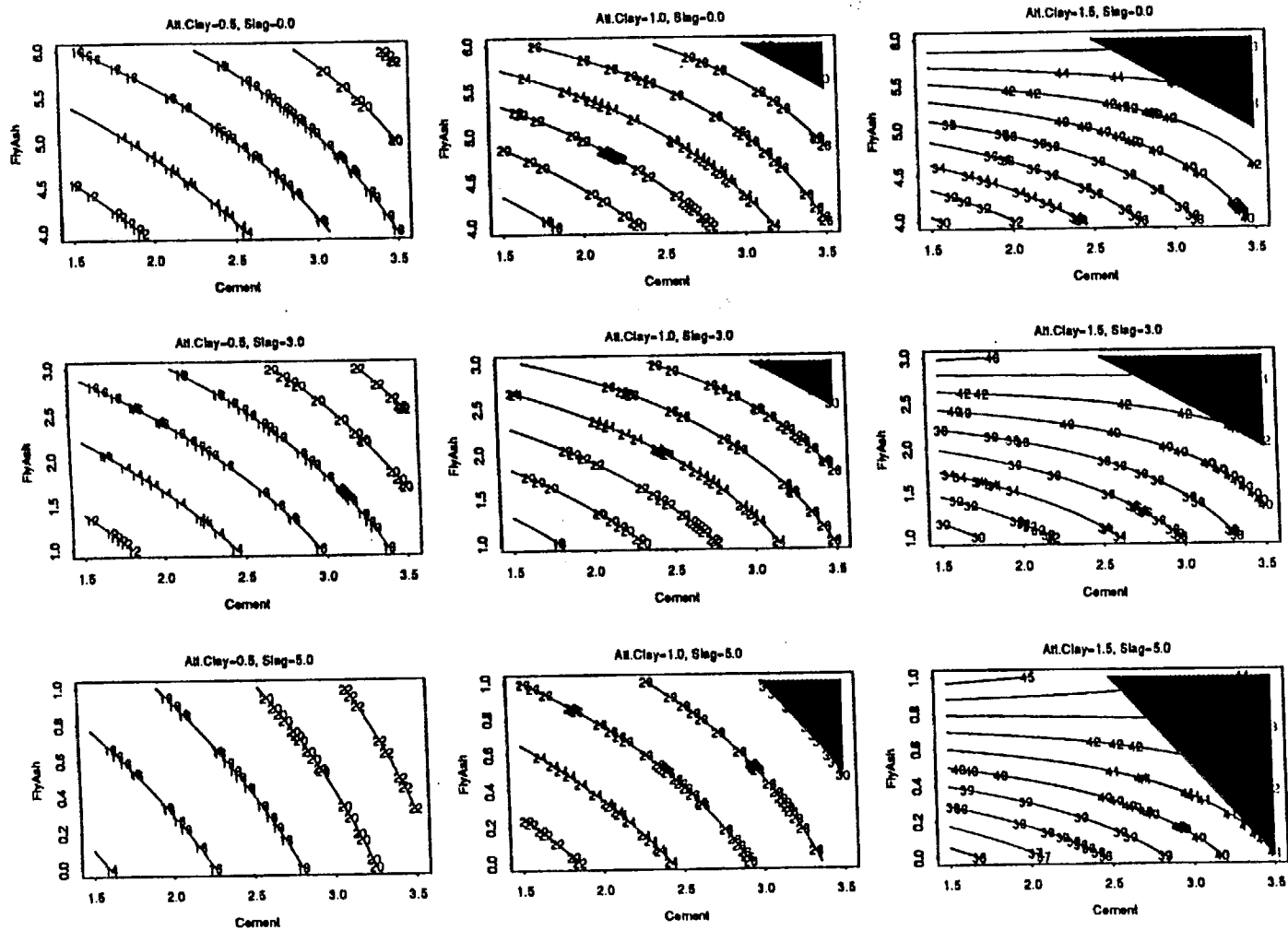


Fig. 4. Surface response contour plots for the critical flow rate, gallons per minute (units for the ingredients are pounds per gallon). Blacked-out regions indicate areas outside the constrained region.

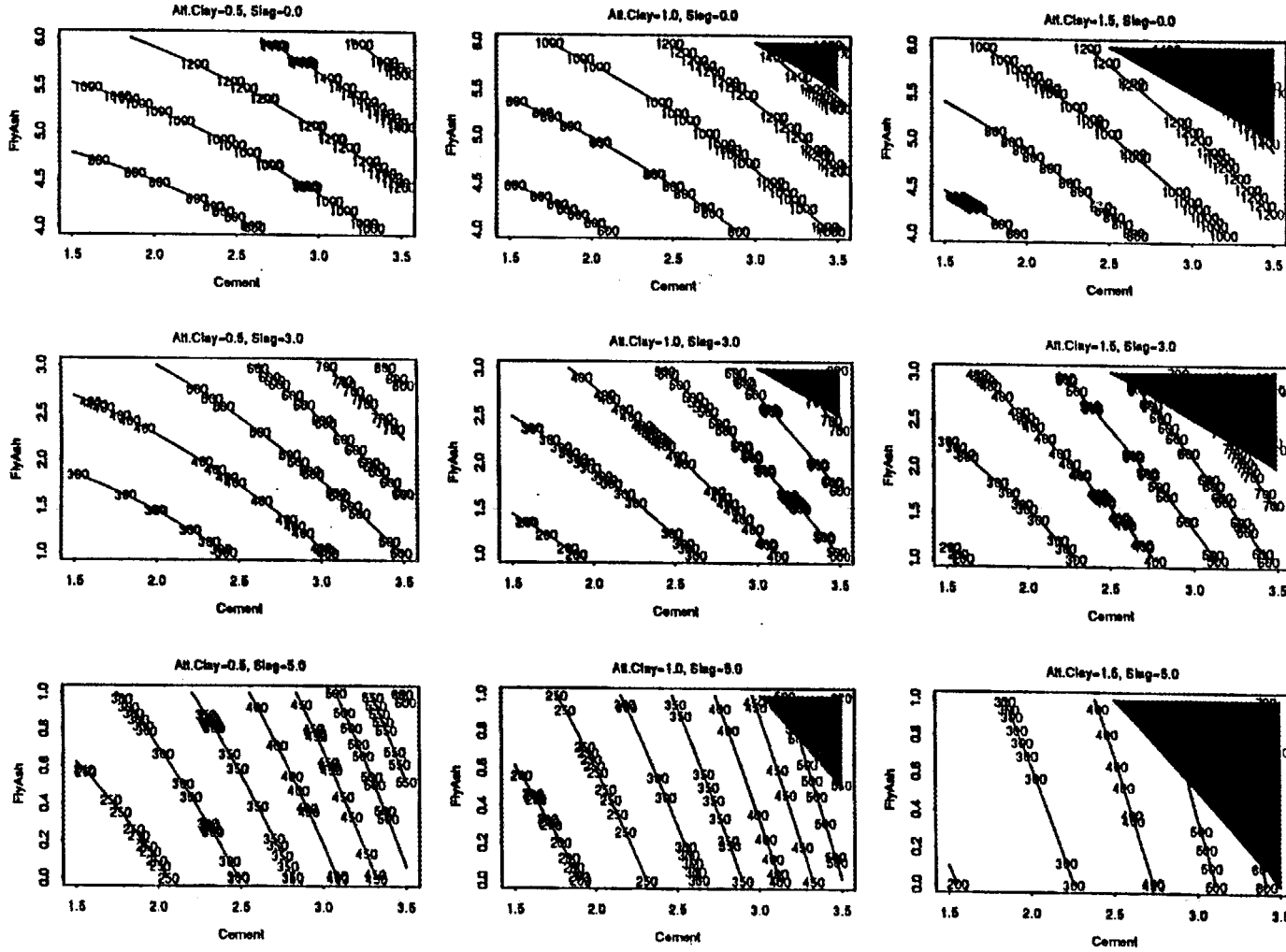


Fig. 5. Surface response contour plots for the corrected unconfined compressive strength, pounds per square inch (units for the ingredients are pounds per gallon). Blacked-out regions indicate areas outside the constrained region.

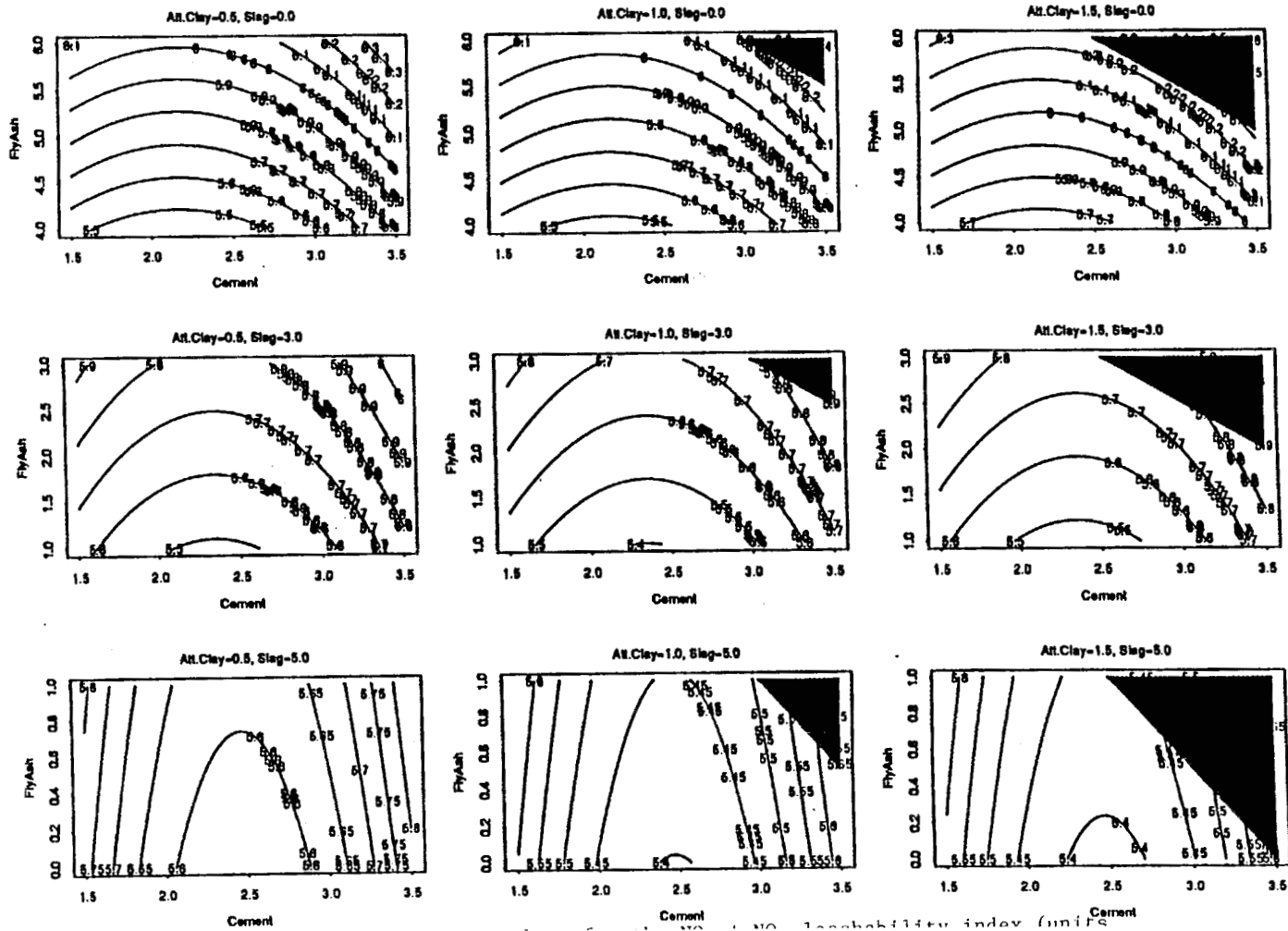


Fig. 6. Surface response contour plots for the $\text{NO}_2 + \text{NO}_3$ leachability index (units for the ingredients are pounds per gallon). Blacked-out regions indicate areas outside the constrained region.

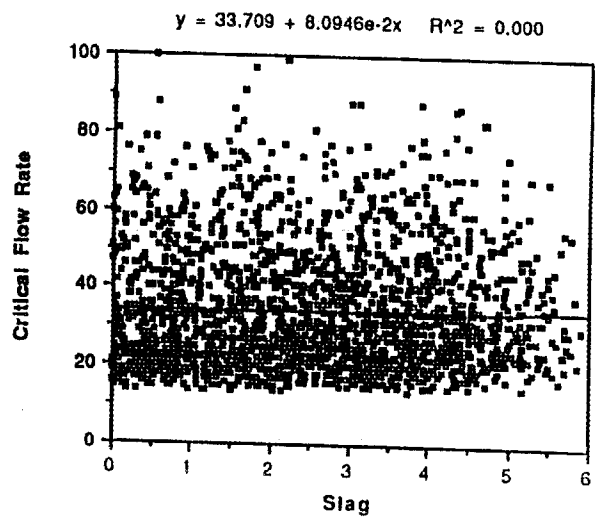
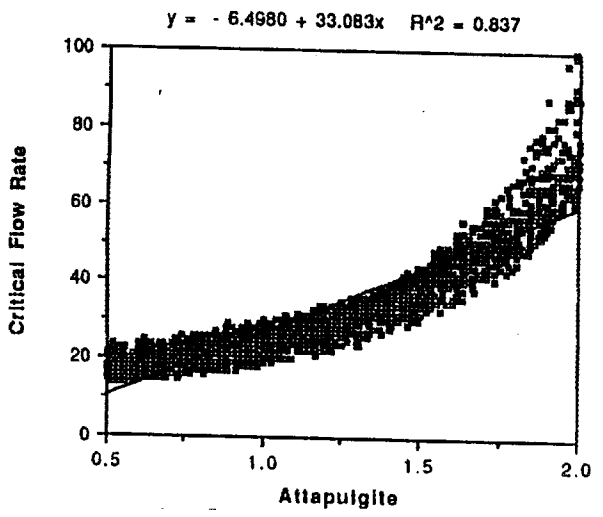
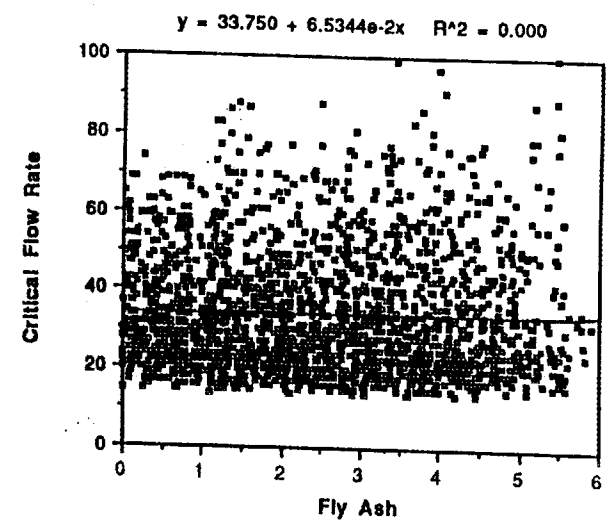
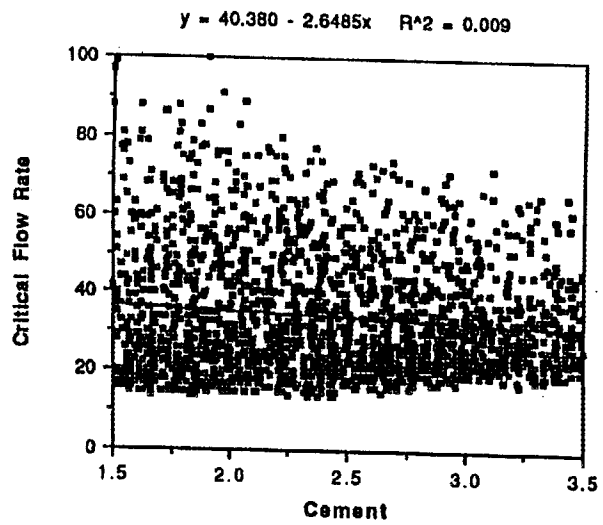


Fig. 7. Predicted critical flow rate, gallons per minute, with composition for the random grouts (units of composition are pounds per gallon).

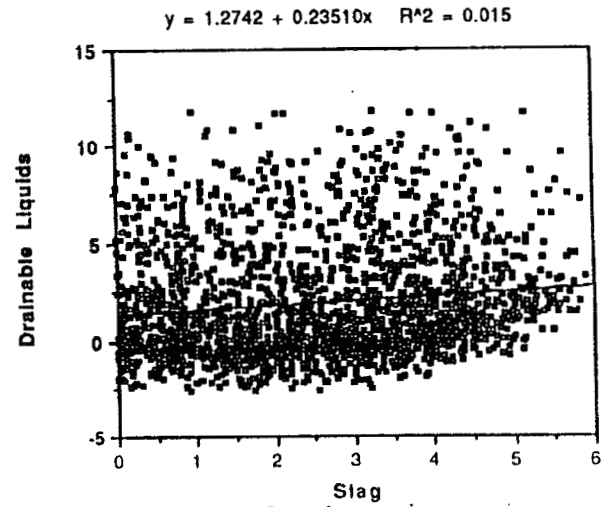
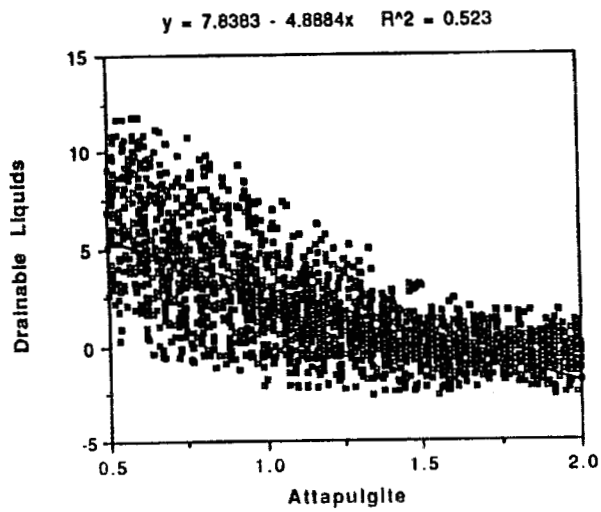
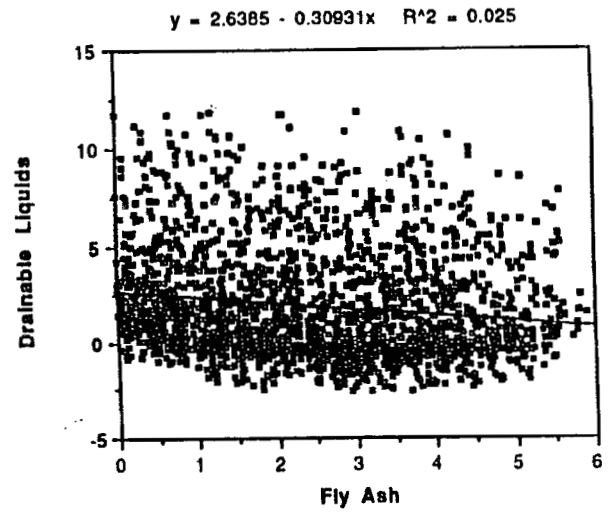
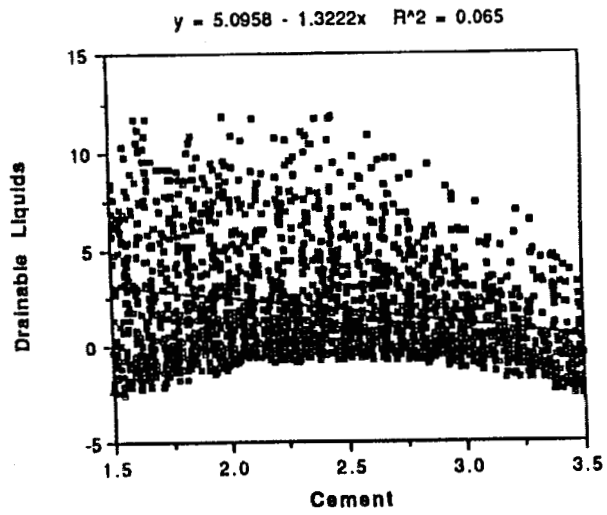


Fig. 8. Predicted freestanding liquid, volume percent, with composition for the random grouts (units of composition are pounds per gallon).

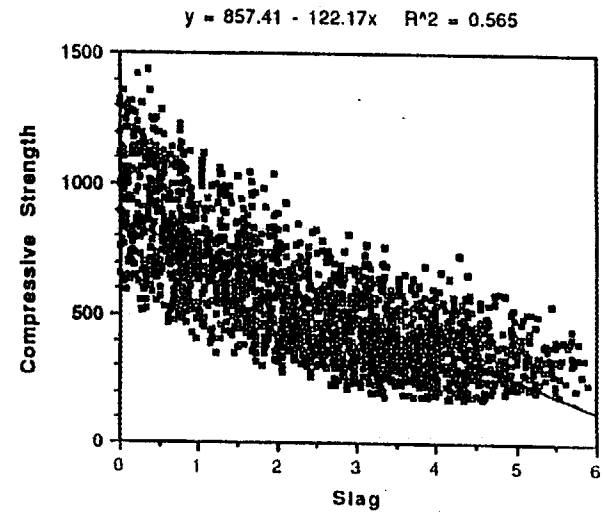
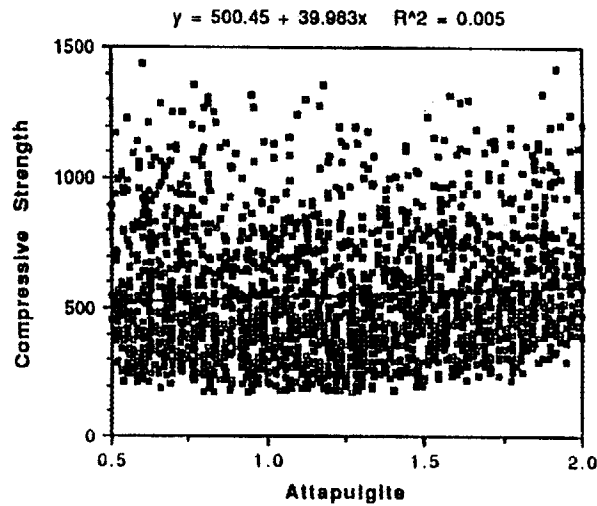
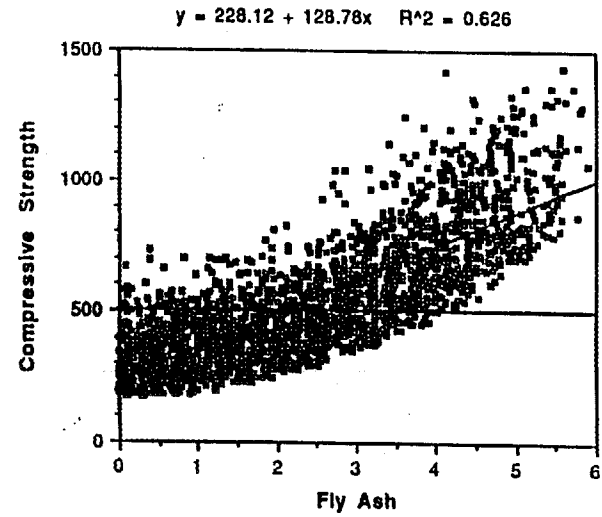
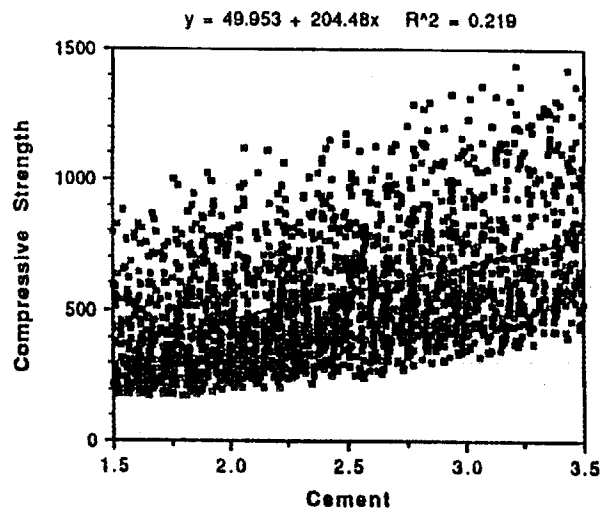


Fig. 9. Predicted corrected unconfined compressive strength, pounds per square inch, with composition for the random grouts (units of composition are pounds per gallon).

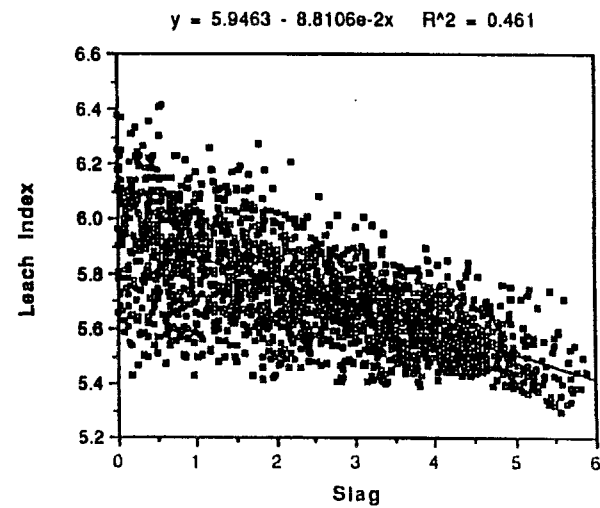
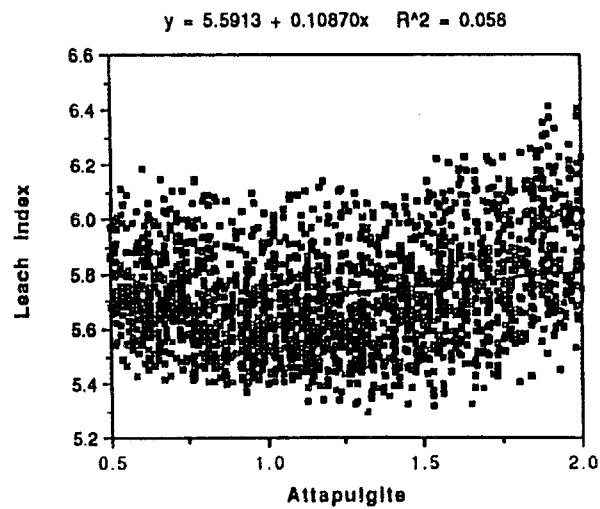
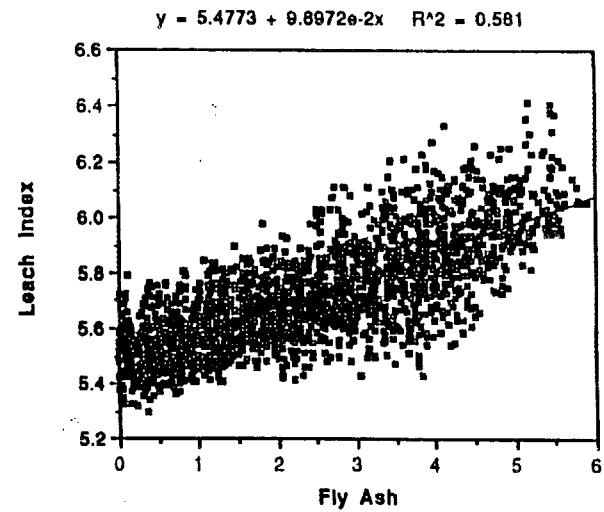
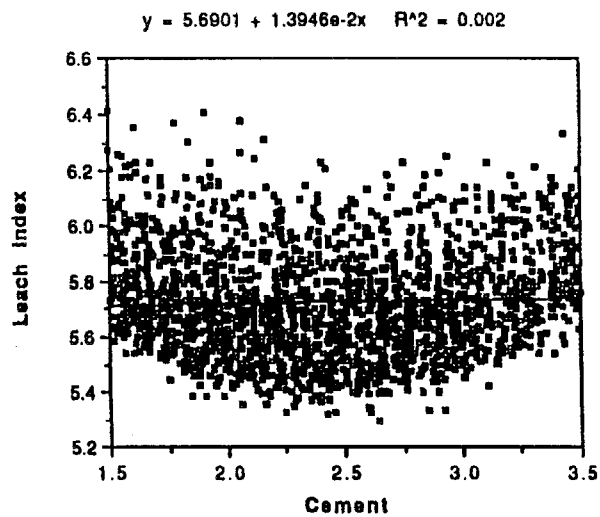


Fig. 10. Predicted $\text{NO}_2 + \text{NO}_3$ leachability index with composition for the random grouts (units of composition are pounds per gallon).

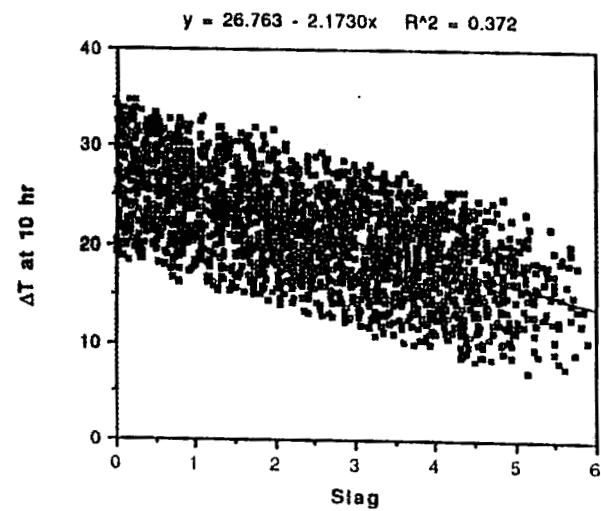
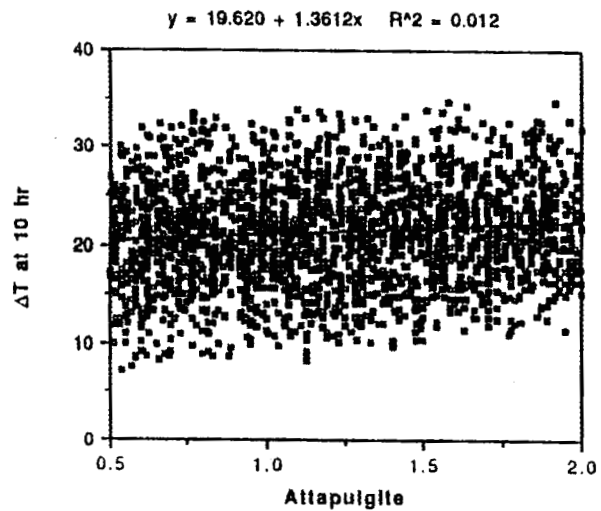
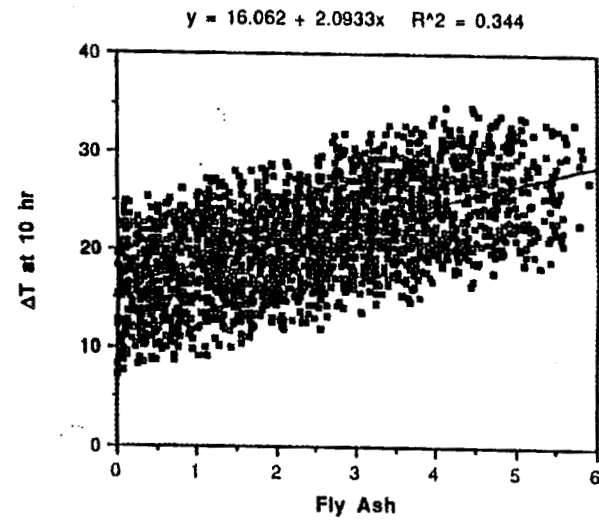
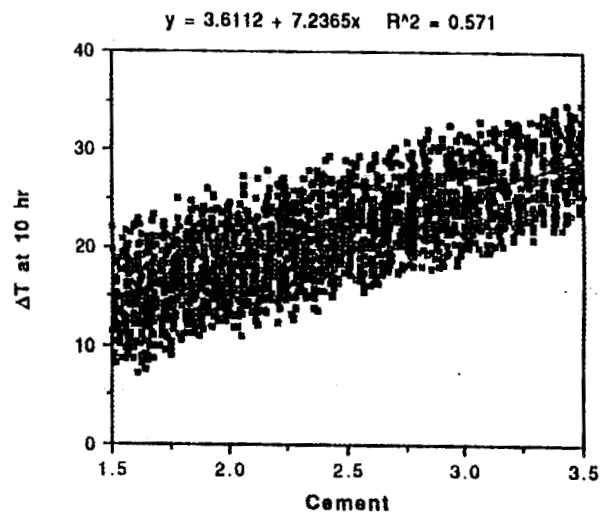


Fig. 11. Predicted adiabatic temperature rise, °C, at 10 h, with composition for the random groups (units of composition are pounds per gallon).

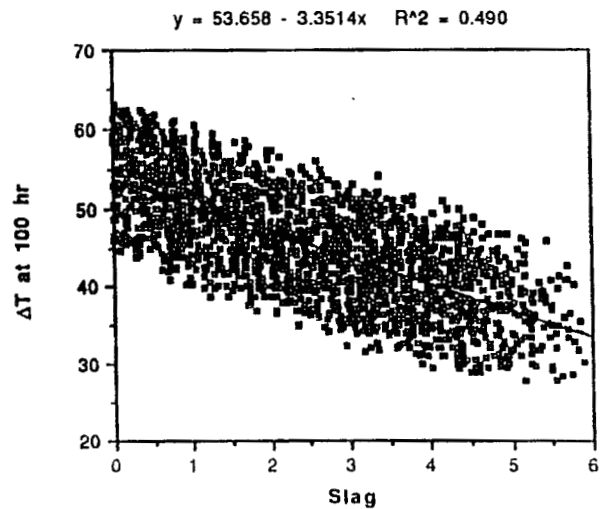
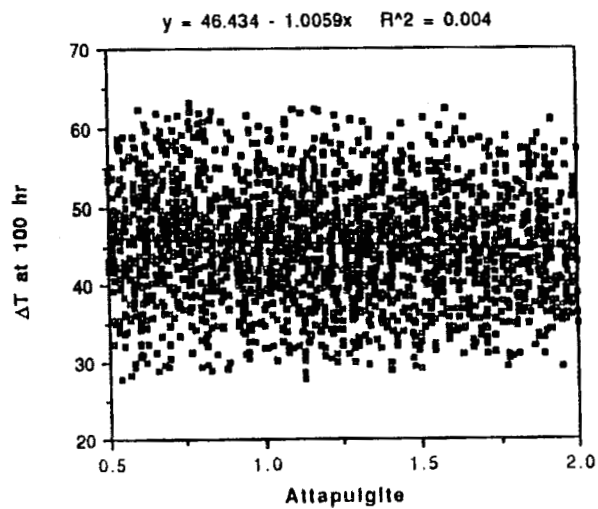
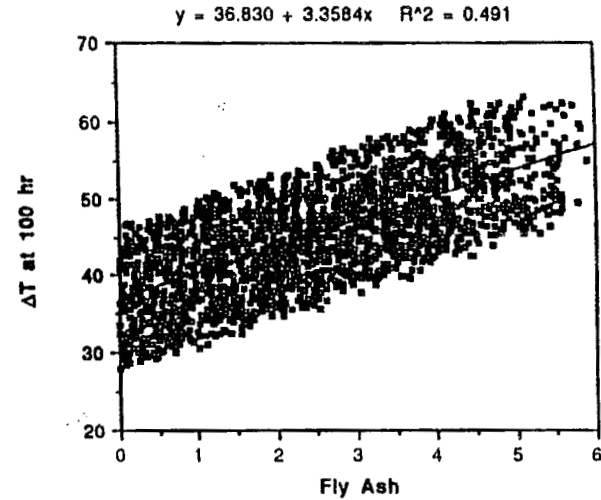
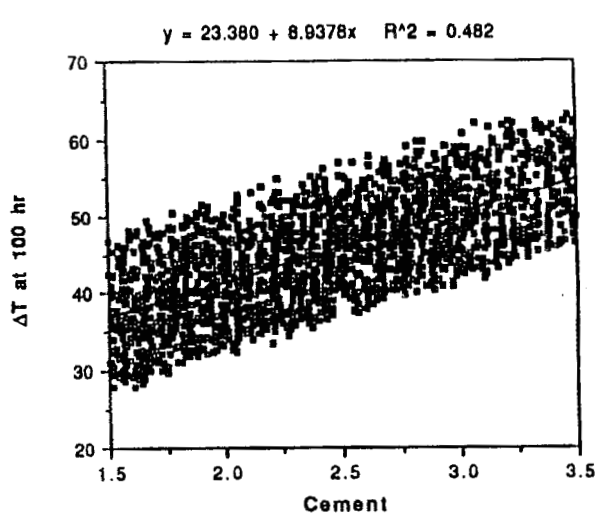


Fig. 12. Predicted adiabatic temperature rise, °C, at 100 h, with composition for the random grouts (units of composition are pounds per gallon).

adjustments to the models are necessary or give confidence that the empirical models are the best for the available data set. The validation results will be issued in a later report.

In addition, the predicted properties are those for laboratory grouts generated using the laboratory procedures. Any grout selected for use in solidifying 106-AN waste must be tested, and is being tested, using conditions more reflective of those expected during field operation. This is being done at PNL and WHC by (1) laboratory-curing the selected surrogate 106-AN grout and changing the temperature with time to approximate the temperature-time history that the grout might experience in the vault, (2) testing the selected grout with actual, rather than surrogate, 106-AN waste, and (3) implementing a pilot-scale pour of the selected grout.

The adiabatic temperatures were the most difficult to measure, and too many of the mixture-experiment grouts could not be extrapolated to a final temperature with confidence to generate a model that predicted this property with confidence. For this reason, the data that were measured with confidence were used to generate models to predict adiabatic temperatures at 10, 24, and 100 h. The temperature at a given time can be used to help select a low-heat evolution formulation even if the final adiabatic temperature cannot be predicted. For this reason, the models can provide no assurance that a criteria on the final adiabatic temperature could be met if such a criteria existed. The temperature limitation that does exist applies to the vault, and processing strategies are being developed to ensure that the vault does not exceed 90°C.

Studying the predicted values inside the constrained region, it became obvious that (1) the entire constrained region was predicted to have a 10-min gel strength of <100 lb_f/100 ft², (2) most grouts in the constrained region with about 2 lb of attapulgite 150 per gallon were predicted to have critical flow rates exceeding 60 gal/min, and (3) most grouts in the constrained region with ≤1.5 lb of attapulgite 150 per gallon were predicted to have critical flow rates <60 gal/min. The attapulgite 150 was restricted to ≤1.5 lb/gal because of these latter two observations. The over 2000 random grouts were scanned for those that met the following criteria:

Critical flow rate	<50 gal/min
Freestanding liquid	<3.0 vol %
28-d unconfined compressive strength	>500 psi
Nitrate + nitrite leachability index	>6
Attapulgite content	<1.5 lb/gal

The freestanding liquid criteria was expanded from 0.5 to 3.0 vol % because processing steps to help cool the curing grout may require a water layer. Using a critical flow rate cutoff of 50 gal/min rather than the criteria value of 60 gal/min ensured conservatism in scanning these grouts. The attapulgite content criteria is not a WHC criteria but was based on the observation of difficulties in measuring the rheology with a Fann viscometer with attapulgite contents above 1.5 lb/gal. From over 2000 random grouts, 106 potential formulations met the above criteria. These 106 formulations are listed in Appendix F.

8.2 RECOMMENDED GROUT FORMULATIONS FOR 106-AN

Table 8 lists the eight grout formulations for 106-AN that were recommended to satisfy the following conditions. Table 9 lists the predicted properties and 95% confidence intervals

Table 8. Recommended grout formulations for 106-AN

Condition No.	Mix ratio (lb/gal)				
	Cement	Fly ash	Clay	GABFS	Total
1	1.74	5.74	1.22	0.00	8.70
2	1.64	5.08	0.74	0.74	8.20
3	1.60	4.70	1.34	0.76	8.40
4	1.62	4.51	1.11	1.28	8.50
5	1.55	1.92	1.04	2.89	7.40
6	3.38	4.90	0.62	0.00	8.90
7	3.10	5.70	1.20	0.00	10.0
8	3.44	3.26	0.65	1.95	9.30

for these grouts. The conditions that the grouts shown in Table 8 satisfy (listed by corresponding condition number) are:

1. Elimination of slag. This would simplify the dry blend, reducing the number of ingredients to three, and benefit the program because of the uncertainties associated with the slag supplier commitments and procurement.
2. Maximization of freestanding liquid to an upper limit of 3 vol %. It was assumed some liquid would be necessary for evaporative cooling.

Table 9. Predicted properties of the recommended 106-AN grouts

Condition No./ prediction interval (%) ^a	Critical flow rate (gal/ min)	Free- standing liquid (vol %)	28-d unconfined compressive strength (psi)	Nitrate + nitrite leach index	Adiabatic temperature increase (°C)		
					10 h	24 h	100 h
1/95	31.3	0.7	916.	6.07	22	38	48
lower	28.3	0.3	754.	5.74	20	36	42
upper	35.0	1.6	1093.	6.40	24	40	54
2/95	19.4	2.9	782.	5.96	18	33	46
lower	17.8	1.2	636.	5.64	15	31	40
upper	21.2	6.8	943.	6.27	20	35	52
3/95	33.8	0.5	632.	5.99	20	34	45
lower	30.5	0.2	501.	5.67	18	32	39
upper	38.2	1.1	779.	6.31	22	37	50
4/95	27.7	0.9	587.	5.95	19	33	45
lower	25.0	0.4	460.	5.62	17	31	39
upper	30.5	2.2	728.	6.21	21	35	50
5/95	21.0	1.7	245.	5.65	15	23	34
lower	19.2	0.7	166.	5.34	13	21	29
upper	22.9	4.0	338.	5.97	17	26	40
6/95	20.8	2.2	1261.	6.00	32	43	61
lower	19.1	0.9	1069.	5.68	30	41	55
upper	22.9	5.3	1468.	6.33	35	46	67
7/95	34.0	0.5	1356.	6.20	34	47	61
lower	30.5	0.2	1154.	5.87	32	45	55
upper	38.2	2.7	1574.	6.53	36	50	67
8/95	22.7	1.8	829.	5.96	31	38	57
lower	20.8	0.7	675.	5.64	29	40	51
upper	25.0	4.2	998.	6.28	33	42	63

^aSee Appendix C for a comparison of prediction and confidence intervals.

3. Control of freestanding liquid at <0.5 vol % to meet existing criteria.
4. Use of lowest heat generation with all other criteria met.
5. Use of lowest heat generation while allowing other properties to fail the existing criteria.

6. Minimization of critical flow rate and maximized heat generation rate. This combination of properties may provide an opportunity to remove the heat during processing, possibly through a slow, continuous pour.
7. Maximization of leachability index.
8. Provision of a large, acceptable operating window. This allows easier process control and greater analytical variability.

These formulations for the above conditions were selected from the greater than 2000 random grouts in Appendix E. All but No. 5 were selected from the subset in Appendix F that meets the criteria listed in Sect. 2 for the grout formulation with the possible exception of heat evolution. Number 5 demonstrates the sacrifices made in the other properties in order to achieve the lowest heat evolution in the constrained region (at least among the over 2000 random grouts scanned). Completely addressing heat evolution for the 106-AN campaign is beyond the scope of this report. Design and administrative controls will be used to supplement the heat reduction accomplished by this work. If further evaluation proves heat evolution cannot be adequately handled during operation, this report provides tools to select the lowest heat-evolving grouts that meet other property requirements.

Scanning the random grout set for the primary condition usually resulted in several potential grouts. To narrow this short list to one grout, the grout with the “best” properties (e.g., lowest heat evolution, strongest, lowest freestanding liquid, largest operating window, etc.) in this short list was selected.

8.3 106-AN FORMULATIONS SELECTED

WHC originally selected the formulation recommended for condition No. 6. This selection was based primarily on the following criteria (listed in order of importance):

1. The grout that releases larger amounts of hydration heat in shorter times. This will permit the removal of as much heat as possible by selected mechanical means. The latter includes pour halts and the use of improved exhausters.
2. The material with the higher 28-d unconfined compressive strength.
3. The material with the higher leach resistances after a 28-d cure.
4. Enough excess liquid left after 28 d to support evaporative cooling.

The above criteria leads to the higher rapid-heat-evolving grouts; thus, the grout selected was a high-heat-evolution grout. This will not be a concern if the mechanical means of cooling will control the temperature below the desired limit. The mechanical cooling capability is currently being evaluated. Another cooler formulation (i.e., the formulation recommended for condition No. 1) has now been selected for the PNL Pilot Scale Test Pours. Formulation No. 6 remains a possible backup at this time. This report presents the tools to respond to problems that may arise, foreseen or unforeseen, during the testing of the selected 106-AN grout formulations.

9. ACKNOWLEDGMENTS

The authors gratefully acknowledge the laboratory and experimental assistance of S. C. Osborne, C. L. Francis, I. L. Morgan, and D. R. Trotter; the manuscript organization and revision assistance of I. Beaty and J. Williams; and the financial support of WHC.

10. REFERENCES

1. E. F. Riebling and J. G. Fadeff, *Grout Formulation Standard Document*, WHC-SD-WM-CSD-003 (rev. 0), Westinghouse Hanford Co., Richland, Wash., October 1991.
2. Dwight K. Smith, *Cementing*, Monograph Vol. 4, Henry L. Doherty Series, rev. ed., Society of Petroleum Engineers, 1990.
3. John A. Cornell, *Experiments with Mixtures*, 2nd ed., Wiley, New York, 1990.
4. G. F. Piepel, *MIXSOFT—Software for the Design and Analysis of Mixture Experiments, Version 2.0*, MIXSOFT—Mixture Experiment Software, Richland, Wash. 1991.
5. W. J. Welch, *ACED—Algorithms for the Construction of Experimental Designs, User's Guide Version 1.6.1*, University of Waterloo, Waterloo, Ontario, Canada, 1987.
6. G. E. P. Box, W. G. Hunter, and J. S. Hunter, *Statistics for Experimenters*, Wiley, New York, 1991.
7. G. E. P. Box and N. R. Draper, *Empirical Model-Building and Response Surfaces*, Wiley, New York, 1987, pp. 288–91.

INTERNAL DISTRIBUTION

- | | | | |
|-------|-------------------|--------|--|
| 1. | J. B. Berry | 19. | S. M. Robinson |
| 2. | W. D. Bostick | 20. | M. K. Savage |
| 3. | C. H. Brown | 21. | J. L. Shoemaker |
| 4. | A. G. Croff | 22-26. | R. D. Spence |
| 5. | T. L. Donaldson | 27. | O. K. Tallent |
| 6. | C. L. Francis | 28. | D. R. Trotter |
| 7. | R. K. Genung | 29. | J. E. Williams |
| 8-12. | T. M. Gilliam | 30. | J. H. Wilson |
| 13. | H. W. Godbee | 31. | Central Research Library |
| 14. | H. M. Henson | 32. | ORNL Y-12 Technical Library,
Document Reference Section |
| 15. | A. P. Malinauskas | 33. | Laboratory Records - RC |
| 16. | E. W. McDaniel | 34-35. | Laboratory Records |
| 17. | I. L. Morgan | 36. | ORNL Patent Section |
| 18. | S. C. Osborne | | |

EXTERNAL DISTRIBUTION

37. C. M. Anderson, Battelle Pacific Northwest Laboratories, Battelle Boulevard, Richland, Washington 99352
38. J. J. Barich, U.S. Environmental Protection Agency, 1200 Sixth Avenue, Seattle, Washington 98101
39. K. C. Burgard, Westinghouse Hanford Company, P.O. Box 1970, Richland, Washington 99352
40. R. O. Lokken, Battelle Pacific Northwest Laboratories, Battelle Boulevard, Richland, Washington 99352
41. R. J. Murkowski, Westinghouse Hanford Company, P.O. Box 1970, Richland, Washington 99352
42. G. F. Piepel, Battelle Pacific Northwest Laboratories, Battelle Boulevard, Richland, Washington 99352
43. E. F. Riebling, Westinghouse Hanford Company, P.O. Box 1970, Richland, Washington 99352
44. J. H. Westsik, Jr., Battelle, Pacific Northwest Laboratories, Battelle Boulevard, Richland, Washington 99352
45. Office of Assistant Manager, Energy Research and Development, DOE-ORO, P.O. Box 2001, Oak Ridge, Tennessee 37831
- 46-47. Office of Scientific and Technical Information, P.O. Box 62, Oak Ridge, Tennessee 37831